Discrete Comput Geom
DOI 10.1007/s00454-016-9832-0

Encoding Toroidal Triangulations

Vincent Despré[1] · **Daniel Gonçalves**[2] · **Benjamin Lévêque**[3]

Received: 12 November 2015 / Revised: 16 September 2016 / Accepted: 27 September 2016

Abstract Poulalhon and Schaeffer introduced an elegant method to linearly encode a planar triangulation optimally. The method is based on performing a special depth-first search algorithm on a particular orientation of the triangulation: the minimal Schnyder wood. Recent progress toward generalizing Schnyder woods to higher genus enables us to generalize this method to the toroidal case. In the plane, the method leads to a bijection between planar triangulations and some particular trees. For the torus we obtain a similar bijection but with particular unicellular maps (maps with only one face).

Keywords Toroidal triangulations · Schnyder woods · Alpha-orientations · Distributive lattices · Poulalhon and Schaeffer's method · Unicellular maps · Bijective encoding

Mathematics Subject Classification 05C10 · 05C30 · 05A19 · 68R10 · 06D99

Editor in Charge: János Pach

Vincent Despré
vincent.despre@gipsa-lab.fr

Daniel Gonçalves
daniel.goncalves@lirmm.fr

Benjamin Lévêque
benjamin.leveque@cnrs.fr

1 GIPSA-Lab, University Grenoble Alpes, Grenoble, France

2 CNRS, LIRMM, University Montpellier, Montpellier, France

3 CNRS, G-SCOP, University Grenoble Alpes, Grenoble, France

Published online: 26 October 2016

1 Introduction

A graph embedded on a surface is called a *map* on this surface if all its faces are homeomorphic to open disks. A map is a triangulation if all its faces have length three. A closed curve on a surface is *contractible* if it can be continuously transformed into a single point. Given a graph embedded on a surface, a *contractible loop* is an edge forming a contractible curve. Two edges of an embedded graph are called *homotopic multiple edges* if they have the same extremities and their union encloses a region homeomorphic to an open disk. In this paper, we restrict ourself to graphs embedded on surfaces that do not have contractible loops nor homotopic multiple edges. Note that this is a weaker assumption, than the graph being *simple*, i.e. not having loops nor multiple edges. In this paper we distinguish cycles from closed walk as cycles have no repeated vertices. A *triangle* of a map is a closed walk of length three enclosing a region that is homeomorphic to an open disk. This region is called the *interior* of the triangle. Note that a triangle is not necessarily a face of the map as its interior may be not empty. Note also that a triangle is not necessarily a cycle since non-contractible loops are allowed. We denote by n the number of vertices, m the number of edges and f the number of faces of a given map.

Poulalhon and Schaeffer introduced in [20] a method (called here PS method for short) to linearly encode a planar triangulation with a binary word of length $\log_2 \binom{4n}{n} \sim n \log_2 \left(\frac{256}{27}\right) \approx 3.2451\, n$ bits. This is asymptotically optimal since it matches the information theory lower bound. The method is the following. Given a planar triangulation G, it considers the minimal *Schnyder wood* of G (that is the orientation where all inner vertices have outdegree 3 and that contains no cycle oriented clockwise). Then a special depth-first search algorithm is applied by "following" ingoing edges and "cutting" outgoing ones. The algorithm outputs a rooted spanning tree with exactly two leaves (also called stems) on each vertex from which the original triangulation can be recovered in a straightforward way. This tree can be encoded very efficiently. A nice aspect of this work, besides its interesting encoding properties, is that the method gives a bijection between planar triangulations and a particular type of plane trees.

Aleardi et al. [3] adapt PS method to encode planar triangulations with boundaries. A consequence is that a triangulation of any oriented surface can be encoded by cutting the surface along non-contractible cycles and see the surface as a planar map with boundaries. This method is a first attempt to generalize PS algorithm to higher genus. The obtained algorithm is asymptotically optimal (in terms of number of bits) but it is not linear, nor bijective.

The goal of this paper is to present a new generalization of PS algorithm to higher genus based on some strong structural properties. Applied on a well chosen orientation of a toroidal triangulation, what remains after the execution of the algorithm is a *unicellular map*, i.e. a map with only one face (which corresponds to the natural generalization of trees when going to higher genus, see [7,8]), that can be encoded optimally using $3.2451\, n$ bits. Moreover, the algorithm can be performed in linear time and leads to a new bijection between toroidal triangulations and a particular type of unicellular maps.

The two main ingredients that make PS algorithm work in an orientation of a planar map are minimality and accessibility of the orientation. *Minimality* means that there is no clockwise cycle. *Accessibility* means that there exists a root vertex such that all the vertices have an oriented path directed toward the root vertex. Given $\alpha : V \to \mathbb{N}$, an orientation of G is an α-orientation if for every vertex $v \in V$ its outdegree $d^+(v)$ equals $\alpha(v)$. The existence and uniqueness of minimal orientations in the plane is given by the following result of Felsner [12] (related to older results of Propp [21] and de Mendez [10]): the set of α-orientations of a given planar map carries a structure of distributive lattice. This gives the existence and uniqueness of a minimal α-orientation as soon as an α-orientation exists. Felsner's result enables several analogues of PS method to other kind of planar maps, see [2,4,11]. In all these cases the accessibility of the considered α-orientations is a consequence of the natural choice of α, like in Poulalhon and Schaeffer's original work [20] where any orientation of the inner edges of a planar triangulation with inner vertices having outdegree 3 is accessible for any choice of root vertex on the outer face. (Note that the conventions may differs in the literature: the role of outgoing and incoming edges are sometimes exchanged and/or the role of clockwise and counterclockwise.)

For higher genus, the minimality can be obtained by the following generalization of Felsner's result. The second author, Knauer and the third author [16] showed that on any oriented surface the set of orientations of a given map having the same homology carries a structure of distributive lattice. Note that α has been removed here since it is captured by the homology (see Sect. 2 for a brief introduction to homology). Note also that this result is equivalent to an older result of Propp [21] where the lattice structure is described in the dual setting. Since this result is very general, there is hope to be able to further generalize PS method to other oriented surfaces. Note that a given map on an oriented surface can have several α-orientations (for the same given α) that are not homologous. So the set of α-orientations of a given map is now partitioned into distributive lattices contrarily to the planar case where there is only one lattice (and thus only one minimal element). In the case of toroidal triangulations we manage to face this problem and maintain a bijection by recent results on the structure of 3-*orientations* of toroidal triangulations (i.e. α-orientation such that $\alpha(v) = 3$ for all vertices v). We identify a special lattice (and thus a special minimal orientation) using the notion of Schnyder woods generalized to the torus by the second and third author in [15] (further generalized in [16], see also [18] for a unified presentation).

The main issue while trying to extend PS algorithm to higher genus is the accessibility. Accessibility toward the outer face is given almost for free in the planar case because of Euler's formula that sums to a strictly positive value. For an oriented surface of genus $g \geq 1$ new difficulties occur. Already in genus 1 (the torus), even if the orientation is minimal and accessible PS algorithm can visit all the vertices but not all the angles of the map because of the existence of non-contractible cycles. We can show that the special minimal orientation that we choose has the nice property that this problem never occurs. In genus $g \geq 2$ things get even more difficult with separating non-contractible cycles that make having accessibility of the vertices already difficult to obtain.

Another problem is to recover the original map after the execution of the algorithm. If what remains after the execution of PS method is a spanning unicellular map then the map can be recovered with the same simple rules as in the plane. Unfortunately for

many minimal orientations the algorithm leads to a spanning unicellular embedded graph that is not a map (the only face is not a disk) and it is not possible to directly recover the original map. Here again, the choice of our special orientation ensures that this never happens.

Finally the method presented here can be implemented in linear time. Clearly the execution of PS algorithm is linear but the difficulty lies in providing the algorithm with the appropriate orientation in input. Computing the minimal Schnyder wood of a planar triangulation can be done in linear time quite easily by using a so-called shelling order (or canonical order, see [17]). Other similar ad-hoc linear algorithms can sometimes be found for other kinds of α-orientations of planar maps (see for example [13, Chap. 3]). Such methods are not known in higher genus. We solve this problems by first computing an orientation in our special lattice and then go down in the lattice to find the minimal orientation. All this can be performed in linear time.

A brief introduction to homology and to the corresponding terminology used in the paper is given in Sect. 2. In Sect. 3, we present the definitions and results we need concerning the generalization of Schnyder woods to the toroidal case. In Sect. 4, we introduce a reformulation of Poulalhon and Schaeffer's original algorithm that is applicable to any orientation of any map on an oriented surface. The main theorem of this paper is proved in Sect. 5, that is, for a toroidal triangulation given with an appropriate root and orientation, the output of the algorithm is a toroidal spanning unicellular map. In Sect. 6, we show how one can recover the original triangulation from the output. This output is then used in Sect. 7 to optimally encode a toroidal triangulation. The linear time complexity of the method is discussed in Sect. 8. In Sect. 9 (resp. Sect. 11), we exhibit a bijection between appropriately rooted toroidal triangulations and rooted (resp. non-rooted) toroidal unicellular maps. To obtain the non-rooted bijection, further structural results concerning the particular Schnyder woods considered in this paper are given in Sect. 10. Finally, a possible generalization to higher genus is discussed in Sect. 12.

2 A Bit of Homology

We need a bit of surface homology of general maps, which we discuss now. The presentation is not standard but it is short and sufficient to fit our needs. For a deeper introduction to homology we refer to [14].

Consider a map G with edge set E, on an orientable surface of genus g, given with an arbitrary orientation of its edges. This fixed arbitrary orientation is implicit and is used to manipulate flows. A *flow* ϕ on G is a vector in $\mathbb{Z}^E$. For any $e \in E$, we denote by ϕ_e the coordinate e of ϕ.

A *walk* W of G is a sequence of edges with a direction of traversal such that the ending point of an edge is the starting point of the next edge. A walk is *closed* if the start and end vertices coincide. A walk has a *characteristic flow* $\phi(W)$ defined by

$$\phi(W)_e := \text{times } W \text{ traverses } e \text{ forward} - \text{times } W \text{ traverses } e \text{ backward}.$$

This definition naturally extends to sets of walks. From now on we consider that a set of walks and its characteristic flow are the same object. We do similarly for oriented subgraphs as they can be seen as sets of walks.

A *facial walk* is a closed walk bounding a face. Let $\mathcal{F}$ be the set of counterclockwise facial walks and let $\mathbb{F} = \langle \phi(\mathcal{F}) \rangle$ the subgroup of $\mathbb{Z}^E$ generated by $\mathcal{F}$. Two flows ϕ, ϕ' are said to be *homologous* if $\phi - \phi' \in \mathbb{F}$. A flow ϕ is 0-homologous if it is homologous to the zero flow, i.e. $\phi \in \mathbb{F}$.

Let $\mathcal{W}$ be the set of *closed* walks and let $\mathbb{W} = \langle \phi(\mathcal{W}) \rangle$ the subgroup of $\mathbb{Z}^E$ generated by $\mathcal{W}$. The group $H(G) = \mathbb{W}/\mathbb{F}$ is the *first homology group* of G. Since $\dim(\mathbb{W}) = m - n + 1$ and $\dim(\mathbb{F}) = f - 1$, Euler's Formula gives $\dim(H(G)) = 2g$. So $H(G) \cong \mathbb{Z}^{2g}$ only depends on the genus of the map. A set $(B_1, \ldots, B_{2g})$ of (closed) walks of G is said to be a *basis for the homology* if $(\phi(B_1), \ldots, \phi(B_{2g}))$ is a basis of $H(G)$.

3 Toroidal Schnyder Woods

Schnyder [22] introduced Schnyder woods for planar triangulations using the following local property:

Given a map G, a vertex v and an orientation and coloring of the edges incident to v with the colors 0, 1, 2, we say that a vertex v satisfies the *Schnyder property* if (see Fig. 1):

- Vertex v has out-degree one in each color.
- The edges $e_0(v)$, $e_1(v)$, $e_2(v)$ leaving v in colors 0, 1, 2, respectively, occur in counterclockwise order.
- Each edge entering v in color i enters v in the counterclockwise sector from $e_{i+1}(v)$ to $e_{i-1}(v)$ (where $i + 1$ and $i - 1$ are understood modulo 3).

Given a planar triangulation G, a (*planar*) *Schnyder wood* of G is an orientation and coloring of the inner edges of G with the colors 0, 1, 2, where each inner vertex v satisfies the *Schnyder property*. In [15,16] (see also the HDR thesis of the third author [18]) a generalization of Schnyder woods for higher genus has been proposed. Since this paper deals with triangulations of the torus only, we use a simplified version of the definitions and results from [15,16,18]).

The definition of Schnyder woods for toroidal triangulations is the following. Given a toroidal triangulation G, a (*toroidal*) *Schnyder wood* of G is an orientation and coloring of the edges of G with the colors 0, 1, 2, where each vertex satisfies the Schnyder property (see Fig. 2 for an example). The three colors 0, 1, 2 are completely symmetric in the definition, thus we consider that two Schnyder woods that are obtained one

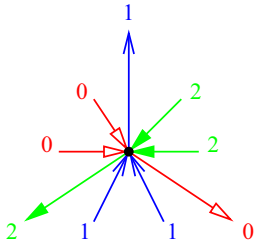

Fig. 1 The Schnyder property. The correspondence between *red*, *blue*, *green* and 0, 1, 2 and the *arrow shapes* used here serves as a convention for all figures in the paper

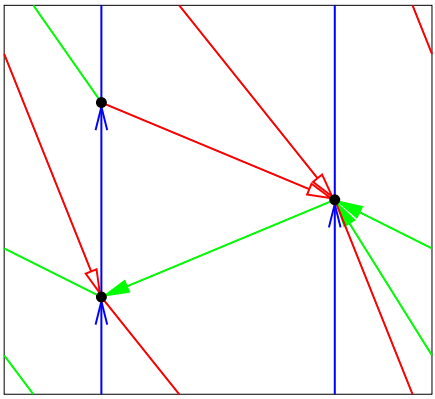

Fig. 2 A Schnyder wood of a toroidal triangulation (opposite sides are identified in order to form a torus)

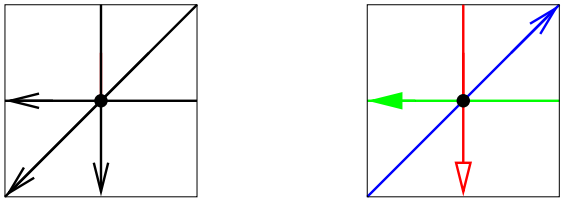

Fig. 3 Two different orientations of a toroidal triangulation. Only the one on the *right* corresponds to a Schnyder wood

from the other by a (cyclic) permutation of the colors are in fact the same object. We consider that a Schnyder wood and its underlying orientation are the same object since one can easily recover a coloring of the edges in a greedy way (by choosing the color of an edge arbitrarily and then satisfying the Schnyder property at every vertex).

Note that the situation is quite different from the planar case. In a Schnyder wood of a toroidal triangulation, each vertex has exactly one outgoing arc in each color, so there are monochromatic cycles contrarily to the planar case (one can show that these monochromatic cycles are non-contractible). Moreover the graph induced by one color is not necessarily connected. Also, by a result of de Fraysseix and de Mendez [9], there is a bijection between orientations of the internal edges of a planar triangulation where every inner vertex has outdegree 3 and Schnyder woods. Thus, in the planar case, any orientation with the proper outdegrees corresponds to a Schnyder wood. This is not true for toroidal triangulations since there exists 3-orientations that do not correspond to a Schnyder wood (see Fig. 3).

A Schnyder wood of a toroidal triangulation is said to be *crossing*, if for each pair i, j of different colors, there exists a monochromatic cycle of color i intersecting a monochromatic cycle of color j. The existence of crossing Schnyder woods is proved in [15, Thm. 1] (note that in [15] the crossing property is included in the definition of Schnyder woods, see [18] for a unified presentation):

Theorem 1 [15] *A toroidal triangulation admits a crossing Schnyder wood.*

Figure 4 depicts two different Schnyder woods of the same graph where just the one on the left is crossing (on the right case the red and green monochromatic cycles do not intersect, we say that the Schnyder wood is "half-crossing" since blue crosses

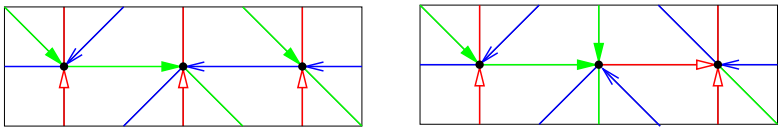

Fig. 4 A crossing and an half-crossing Schnyder wood

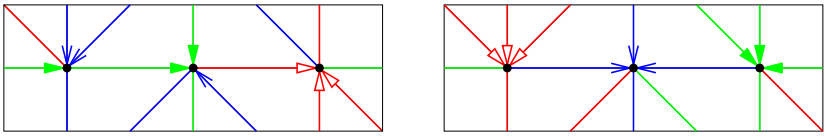

Fig. 5 Non-crossing Schnyder woods

both green and red, see [16,18] for a formal definition). Note that the Schnyder wood on the right is obtained from the one on the left by flipping a clockwise triangle into a counterclockwise triangle.

Consider a toroidal triangulation G given with a crossing Schnyder wood. Let D_0 be the corresponding 3-orientation of G. Let $O(G)$ be the set of all the orientations of G that are homologous to D_0. A consequence of [16] is that all the crossing Schnyder woods of G are homologous to each other. So $O(G)$ contains all the crossing Schnyder woods of G. Thus the definition of $O(G)$ does not depend on the particular choice of D_0 and thus it is uniquely defined. Another consequence of [16] is that every orientation of $O(G)$ corresponds to a Schnyder wood. Thus we call the elements of $O(G)$ the *homologous-to-crossing Schnyder woods* (or *HTC Schnyder woods* for short). Note that all the crossing Schnyder woods are HTC.

Figure 5 gives an example of an HTC Schnyder wood that is not crossing and a Schnyder woods that is not HTC. The example on the left is obtained from the crossing Schnyder wood of Fig. 4 by flipping two triangles (one to obtain the half-crossing Schnyder wood of Fig. 4 and then another one flipped from counterclockwise to clockwise). Thus it is HTC since the difference with a crossing Schnyder wood is a 0-homologous oriented subgraph. The example on the right of Fig. 5 is obtained from the crossing Schnyder wood of Fig. 4 by reversing the three vertical red monochromatic cycles. The union of these three cycles is not a 0-homologous oriented subgraph, thus the resulting orientation is not HTC.

Let us now define briefly what a lattice is. Consider a partial order $\leq$ on a set S. Given two elements x, y of S, let $m(x, y)$ (resp. $M(x, y)$) be the set of elements z of S such that $z \leq x$ and $z \leq y$ (resp. $z \geq x$ and $z \geq y$). If $m(x, y)$ (resp. $M(x, y)$) is not empty and admits a unique maximal (resp. minimal) element, we say that x and y admit a *meet* (resp. a *join*), noted $x \vee y$ (resp. $x \wedge y$). Then $(S, \leq)$ is a *lattice* if any pair of elements of S admits a meet and a join. Thus in particular a lattice has a unique minimal (resp. maximal) element. A lattice is *distributive* if the two operators $\vee$ and $\wedge$ are distributive on each other.

It is proved in [16] that on any oriented surface the set of orientations of a given map having the same homology carries a structure of distributive lattice for a particular order defined below. Thus in particular the set of HTC Schnyder woods carries a structure of distributive lattice.

Let us define an order on the orientations of G. For that purpose, choose an arbitrary face f_0 of G and let F_0 be its counterclockwise facial walk (this choice of a particular face corresponds to the choice of the outer face in the planar case). Let $\mathcal{F}$ be the set of counterclockwise facial walks of G and $\mathcal{F}' = \mathcal{F} \setminus F_0$. We say that a 0-homologous oriented subgraph T of G is *counterclockwise* (resp. *clockwise*) w.r.t. f_0, if its characteristic flow can be written as a combination with positive (resp. negative) coefficients of characteristic flows of $\mathcal{F}'$, i.e. $\phi(T) = \sum_{F \in \mathcal{F}'} \lambda_F \phi(F)$, with $\lambda \in \mathbb{N}^{|\mathcal{F}'|}$ (resp. $-\lambda \in \mathbb{N}^{|\mathcal{F}'|}$). Given two orientations D and D' of G, let $D \setminus D'$ denote the subgraph of D induced by the edges that are not oriented as in D'. We set $D \leq_{f_0} D'$ if and only if $D \setminus D'$ is counterclockwise. In [16, Thm. 7] the following is proved:

Theorem 2 [16] *$(O(G), \leq_{f_0})$ is a distributive lattice.*

Since $(O(G), \leq_{f_0})$ is a distributive lattice, it has a unique minimal element. The following lemma gives a property of this minimum that is essential to apply Poulalhon and Schaeffer's method.

Lemma 1 *The minimal element of $(O(G), \leq_{f_0})$ is the only HTC Schnyder wood that contains no clockwise (non-empty) 0-homologous oriented subgraph w.r.t. f_0.*

Proof Let $D_{\min}$ be the minimal element of $(O(G), \leq_{f_0})$. Suppose by contradiction that $D_{\min}$ contains a clockwise non-empty 0-homologous oriented subgraph T w.r.t. f_0. The orientation of G obtained from $D_{\min}$ by reversing all the edges of T gives an orientation $D \in O(G)$ such that $T = D_{\min} \setminus D$. Furthermore, by definition of $\leq_{f_0}$, we have $D \leq_{f_0} D_{\min}$, a contradiction to the minimality of $D_{\min}$. So $D_{\min}$ contains no clockwise non-empty 0-homologous oriented subgraph w.r.t. f_0.

We now show that this characterizes $D_{\min}$. For any $D \in O(G)$, distinct from $D_{\min}$, we have $D_{\min} \leq_{f_0} D$. Thus $T = D \setminus D_{\min}$ is a non-empty clockwise 0-homologous oriented subgraph of D. □

The crossing Schnyder wood of Fig. 6 is the minimal HTC Schnyder wood for the choice of f_0 corresponding to the shaded face. This example is used in the next sections to illustrate Poulalhon and Schaeffer's method.

The two HTC Schnyder woods of Fig. 4 are not minimal (for any choice of special face f_0) since they contain several triangles that are oriented clockwise. On the contrary, the HTC Schnyder wood of Fig. 5 is minimal w.r.t to its only face oriented clockwise. These examples shows that the minimal HTC Schnyder wood is not always crossing.

We define the dual orientation D^* of an orientation D of G as an orientation of the edges of the dual map G^* of G satisfying the following rule: the dual e^* of an edge e goes from the face on the left of e to the face on the right of e. The following lemma gives the key property of HTC Schnyder woods that we need in this paper:

Lemma 2 *If D is an orientation corresponding to an HTC Schnyder wood, then the dual orientation D^* contains no oriented non-contractible cycle.*

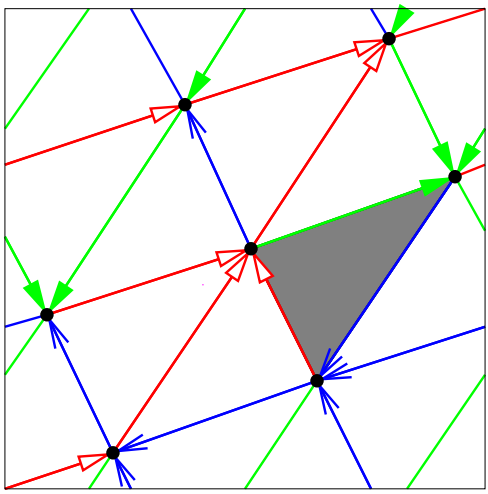

Fig. 6 The minimal HTC Schnyder wood of K_7 w.r.t. the shaded face

Proof We first prove the property for a crossing Schnyder wood and then show that it is stable by reversing a 0-homologous oriented subgraph. Thus it is true for all HTC Schnyder woods.

Consider a crossing Schnyder wood of G by Theorem 1 and let D_0 be the corresponding orientation. For $i \in \{0, 1, 2\}$, let C_i be a monochromatic cycle of color i. In a crossing Schnyder wood, the monochromatic cycles are not contractible and any two monochromatic cycles of different colors are not homologous and intersecting [15]. Thus for any $i \in \{0, 1, 2\}$, the two cycles C_{i-1} and C_{i+1} generate the homology of the torus with respect to $\mathbb{Q}$. That is, for any curve C and $i \in \{0, 1, 2\}$, there exists $(k, k_{i-1}, k_{i+1}) \in \mathbb{Z}^3$, $k \neq 0$, such that kC is homologous to $k_{i-1}B_{i-1} + k_{i+1}B_{i+1}$. By the Schnyder property, the cycle C_{i-1} is crossing C_i (maybe several time) from left to right so there exists $\alpha_1, \alpha_2, \alpha_3 \in \mathbb{N}$, such that $\sum \alpha_i C_i$ is 0-homologous. Thus for any curve C there exists $i \in \{0, 1, 2\}$, $(k, k_{i-1}, k_{i+1}) \in \mathbb{N}^3$, $k \neq 0$, $k_{i-1} \neq 0$, such that kC is homologous to $k_{i-1}B_{i-1} + k_{i+1}B_{i+1}$.

Suppose now by contradiction that D_0^* contains an oriented non-contractible cycle C^*. Let $i \in \{0, 1, 2\}$, $(k, k_{i-1}, k_{i+1}) \in \mathbb{N}^3$, $k \neq 0$, $k_{i-1} \neq 0$, such that kC^* is homologous to $k_{i-1}C_{i-1} + k_{i+1}C_{i+1}$. Then C_{i+1} is crossing C^* at least once from left to right, contradicting the fact that C^* is an oriented cycle of D_0^*. So D_0^* contains no oriented non-contractible cycle.

Consider now a HTC Schnyder wood of G and let D be the corresponding orientation. Since D and D_0 are both element of $O(G)$ they are homologous to each other. Let T be the 0-homologous oriented subgraph of D such that $T = D \setminus D_0$. Thus D_0 is obtained from D by reversing the edges of T.

Suppose by contradiction that D^* contains an oriented non-contractible cycle C^*. The oriented subgraph T is 0-homologous thus it intersects C^* exactly the same number of time from right to left than from left to right. Since C^* is oriented foward, T cannot intersect it from left to right. So T does not intersect C^* at all. Thus reversing T to go from D to D_0 does not affect C^*. Thus C^* is an oriented non-contractible cycle of D_0^*, a contradiction. □

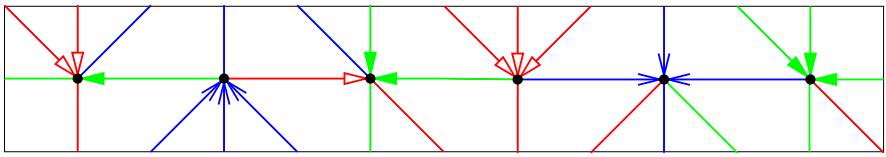

Fig. 7 A Schnyder wood that is not HTC but contains no oriented non-contractible cycle in the dual

For the non-HTC Schnyder wood of Fig. 5, one can see that there is an horizontal oriented non-contractible cycle in the dual, so it does not satisfy the conclusion of Lemma 2. Note that this property is not a characterization of being HTC. Figure 7 is a Schnyder wood that is not HTC but satisfies the conclusion of Lemma 2 (we leave the reader check that this Schnyder wood is not HTC, it will be easier after Sect. 9 and the definition of γ).

4 Poulalhon and Schaeffer's Algorithm on Oriented Surfaces

In this section we introduce a reformulation of Poulalhon and Schaeffer's original algorithm. This version is more general in order to be applicable to any orientation of any map on an oriented surface. The execution slightly differs from the original formulation, even on planar triangulations. In [20], the authors first delete some outer edges of the triangulation before executing the algorithm. We do not consider some edges to be special here since we want to apply the algorithm on any surface but the core of the algorithm is the same. We show general properties of the algorithm in this section before considering toroidal triangulations in the forthcoming sections.

ALGORITHM PS

INPUT : An oriented map G on an oriented surface S, a root vertex v_0 and a root edge e_0 incident to v_0.

OUTPUT : A graph U with stems, embedded on the oriented surface S.

The algorithm explores some of the edges of the map, marking one edge on each iteration.

1. Let $v := v_0$, $e := e_0$, $U := \emptyset$, none of the edges is marked.
2. Let v' be the extremity of e different from v.

Case 1 e is non-marked and entering v. Add e to U and let $v := v'$.
Case 2 e is non-marked and leaving v. Add a stem to U incident to v and corresponding to e.
Case 3 e is already marked and entering v. Do nothing.
Case 4 e is already marked and leaving v. Let $v := v'$.

3. Mark e.
4. Let e be the next edge around v in counterclockwise order after the current e.
5. While $(v, e) \neq (v_0, e_0)$ go back to 2.
6. Return U.

We insist on the fact that the output of ALGORITHM PS is a graph embedded on the same surface as the input map but that this embedded graph is not necessarily a map

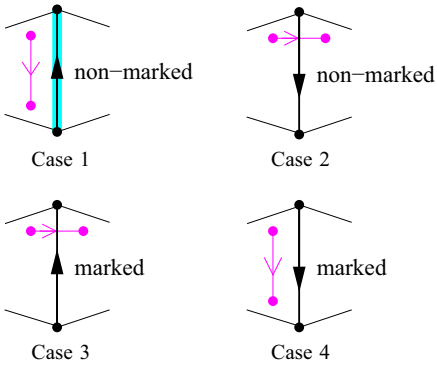

Fig. 8 The four cases of ALGORITHM PS

(i.e some faces may not be homeomorphic to open disks). In the following section we show that in our specific case the output U is a unicellular map on the contrary to some examples presented later on (see Fig. 14).

Consider any oriented map G on an oriented surface given with a root vertex v_0 and a root edge e_0 incident to v_0. When ALGORITHM PS is considering a couple (v, e) we see this like it is considering the angle at v that is just before e in counterclockwise order. The particular choice of v_0 and e_0 is thus in fact a particular choice of a root angle a_0 that automatically defines a root vertex v_0, a root edge e_0, as well as a root face f_0. From now on we consider that the input of ALGORITHM PS is an oriented map plus a root angle (without specifying the root vertex, face and edge).

The *angle graph* of G, is the graph defined on the angles of G and where two angles are adjacent if and only if they are consecutive around a vertex or around a face. An execution of ALGORITHM PS can be seen as a walk in the angle graph. Figure 8 illustrates the behavior of the algorithm corresponding to Case 1–4. In each case, the algorithm is considering the angle in top left position and depending on the marking of the edge and its orientation the next angle that is considered is the one that is the end of the magenta arc of the angle graph. The cyan edge of Case 1 represents the edge that is added to U by the algorithm. The stems of U added in Case 2 are not represented in cyan, in fact we will represent them later by an edge in the dual. Indeed seeing the execution of ALGORITHM PS as a walk in the angle graph enables us to show that ALGORITHM PS behaves exactly the same in the primal or in the dual map (as explained later).

In Fig. 9, we give an example of an execution of ALGORITHM PS on the orientation corresponding to the minimal HTC Schnyder wood of K_7 of Fig. 6.

Let a be a particular angle of the map G. It is adjacent to four other angles in the *angle graph* (see Fig. 10). Let v, f be such that a is an angle of vertex v and face f. The *next-vertex* (resp. *previous-vertex*) angle of a is the angle appearing just after (resp. before) a in counterclockwise order around v. Similarly, the *next-face* (resp. *previous-face*) angle of a is the angle appearing just after (resp. before) a in clockwise order around f. These definitions enable one to orient consistently the edges of the angle graph like in Fig. 10 so that for every oriented edge (a, a'), a' is a next-vertex or next-face angle of a.

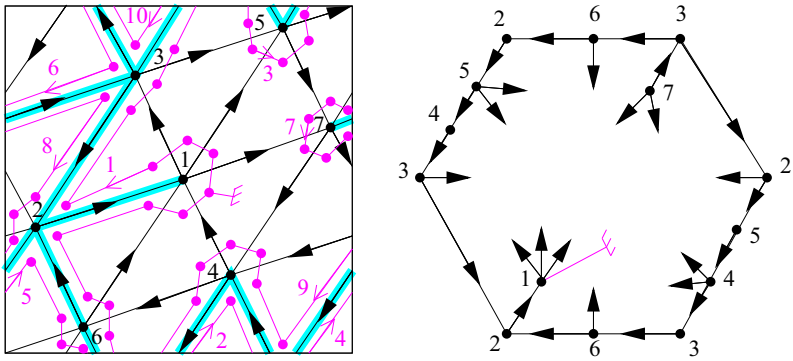

Fig. 9 An execution of ALGORITHM PS on K_7 given with the orientation corresponding to the minimal HTC Schnyder wood of Fig. 6. Vertices are numbered in *black*. The root angle is identified by a root symbol and chosen in the face for which the orientation is minimal (i.e. the *shaded face* of Fig. 6). The *magenta arrows* and numbers are here to help the reader to follow the cycle in the angle graph. The output U is a toroidal unicellular map, represented here as an hexagon where the opposite sides are identified.

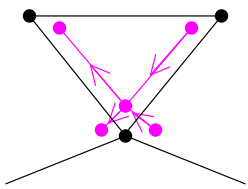

Fig. 10 Orientation of the edges of the angle graph

The different cases depicted in Fig. 8 show that an execution of ALGORITHM PS is just an oriented walk in the angle graph (i.e. a walk that is following the orientation of the edges described in Fig. 10). The condition in the while loop ensures that when the algorithm terminates, this walk is back to the root angle. The following proposition shows that the algorithm actually terminates:

Proposition 1 *Consider an oriented map G on an oriented surface and a root angle a_0. The execution of* ALGORITHM PS *on (G, a_0) terminates and corresponds to a cycle in the angle graph.*

Proof We consider the oriented walk W in the angle graph corresponding to the execution of ALGORITHM PS . Note that W may be infinite. The walk W starts with a_0, and if it is finite it ends with a_0 and contains no other occurrence of a_0 (otherwise the algorithm should have stopped earlier). Toward a contradiction, suppose that W is not simple (i.e. some angles different from the root angle a_0 are repeated). Let $a \neq a_0$ be the first angle along W that is met for the second time. Let a_1, a_2 be the angles appearing before the first and second occurrence of a in W, respectively. Note that $a_1 \neq a_2$ by the choice of a.

If a_1 is the previous-vertex angle of a, then a_2 is the previous-face angle of a. When the algorithm considers a_1, none of a and a_2 are already visited, thus edge e is not marked. Since the execution then goes to a after a_1, we are in Case 2 and the edge e

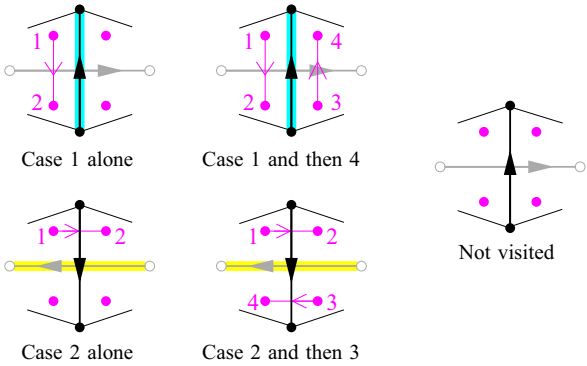

Fig. 11 The different cases of ALGORITHM PS seen in a dual way. The number of the angles gives the order in which the algorithm visits them (unvisited angles are not numbered). The edges of P and Q are respectively *cyan* and *yellow*

between a and a_1 is oriented from v, where v is the vertex incident to a. Afterward, when the algorithm reaches a_2, Case 3 applies and the algorithm cannot go to a, a contradiction. The case where a_1 is the previous-face angle of a is similar.

So W is simple. Since the angle graph is finite, W is finite. So the algorithm terminates, thus W ends on the root angle and W is a cycle. □

In the next section we see that in some particular cases the cycle in the angle graph corresponding to the execution of PS algorithm (Proposition 1) can be shown to be Hamiltonian like in Fig. 9.

By Proposition 1, an angle is considered at most once by ALGORITHM PS. This implies that the angles around an edge can be visited in different ways depicted in Fig. 11. Consider an execution of ALGORITHM PS on G. Let C be the cycle formed in the angle graph by Proposition 1. Let P be the set of edges of the output U (without the stems) and Q be the set of dual edges of edges of G corresponding to stems of U. These edges are represented in Fig. 11 in cyan for P and in yellow for Q. They are considered with their orientation (recall that the dual edge e^* of an edge e goes from the face on the left of e to the face on the right of e). Note that C does not cross an edge of P or Q, and moreover P and Q do not intersect (i.e. an edge can be in P or its dual in Q but both cases cannot happen).

One can remark that the cases of Fig. 11 are dual of each other. One can see that ALGORITHM PS behaves exactly the same if applied on the primal map or on the dual map. The only modifications to make is to start the algorithm with the face f_0 as the root vertex, the dual of edge e_0 as the root edge and to replace counterclockwise by clockwise at Line 4. Then the cycle C formed in the angle graph is exactly the same and the output is Q with stems corresponding to P (instead of P with stems corresponding to Q). Note that this duality is also illustrated by the fact that the minimality of the orientation of G w.r.t. the root face is nothing else than the accessibility of the dual orientation toward the root face. Indeed, a clockwise 0-homologous oriented subgraph of G w.r.t f_0 corresponds to a directed cut of the dual where all the edges are oriented from the part containing f_0. The following lemma shows the connectivity of P and Q:

Lemma 3 *At each step of the algorithm, for every vertex v appearing in an edge of P (resp. Q), there is an oriented path from v to v_0 (resp. f_0) consisting only of edges of P (resp. Q). In particular P and Q are connected.*

Proof If at a step a new vertex is reached then it correspond to Case 1 and the corresponding edge is added in P and oriented from the new vertex, so the property is satisfied by induction. As observed earlier the algorithm behaves similarly in the dual map. □

Let $\overline{C}$ be the set of angles of G that are not in C. Any edge of G is bounded by exactly 4 angles. Since C is a cycle, the 4 angles around an edge are either all in C, all in $\overline{C}$ or 2 in each set (see Fig. 11). Moreover, if they are 2 in each set, these sets are separated by an edge of P or an edge of Q. Hence the frontier between C and $\overline{C}$ is a set of edges of P and Q. Moreover this frontier is a union of oriented closed walks of P and of oriented closed walks of Q. In the next section we study this frontier in more details to show that $\overline{C}$ is empty in the case considered there.

5 From Toroidal Triangulations to Unicellular Maps

Let G be a toroidal triangulation. In order to choose appropriately the root angle a_0, we have to consider separating triangles. A *separating triangle* is a triangle that is different from a face of G, that is a triangle whose interior in non empty. We say that an angle is *in the strict interior of a separating triangle* T if it is in the interior of T and not incident to a vertex of T. We choose as root angle a_0 any angle that is not in the strict interior of a separating triangle. One can easily see that such an angle a_0 always exists. Indeed the interiors of two triangles are either disjoint or one is included in the other. So, the angles that are incident to a triangle whose interior is maximal by inclusion satisfy the property.

A subgraph of a graph is *spanning* if it is covering all the vertices. The main result of this section is the following theorem (see Fig. 9 for an example):

Theorem 3 *Consider a toroidal triangulation G, a root angle a_0 that is not in the strict interior of a separating triangle and the orientation of the edges of G corresponding to the minimal HTC Schnyder wood w.r.t. the root face f_0 containing a_0. Then the output U of* ALGORITHM PS *applied on (G, a_0) is a toroidal spanning unicellular map.*

The choice of a root angle that is not in the interior of a separating triangle is necessary to be able to use Poulalhon and Schaeffer method. Indeed, in a 3-orientation of a toroidal triangulation, by Euler's formula, all the edges that are incident to a separating triangle and in its interior are oriented towards the triangle. Thus if one applies ALGORITHM PS from an angle in the strict interior of a triangle, the algorithm will remain stuck in the interior of the triangle and will not visit all the vertices.

Consider a toroidal triangulation G, a root angle a_0 that is not in the strict interior of a separating triangle and the orientation of the edges of G corresponding to the minimal HTC Schnyder wood w.r.t. the root face f_0 containing a_0. Let U be the output of ALGORITHM PS applied on (G, a_0). We use the same notation as in the previous section: the cycle in the angle graph is C, the set of angles that are not in C is $\overline{C}$, the set of edges of U is P, the dual edges of stems of U is Q.

Lemma 4 *The frontier between C and $\overline{C}$ contains no oriented closed walk of Q.*

Proof Suppose by contradiction that there exists such a walk W. Then along this walk, all the dual edges of W are edges of G oriented from the region containing C toward $\overline{C}$ as one can see in Fig. 11. By Lemma 2, the walk W does not contain any oriented non-contractible cycle. So W contains an oriented contractible cycle W', and then either C is in the contractible region delimited by W', or not. The two case are considered below:

- *C lies in the non-contractible region of W'*

  Then consider the plane map G' obtained from G by keeping only the vertices and edges that lie (strictly) in the contractible region delimited by W'. Let n' be the number of vertices of G'. All the edges incident to G' that are not in G' are entering G'. So in G' all the vertices have outdegree 3 as we are considering 3-orientations of G. Thus the number of edges of G' is exactly $3n'$, contradicting the fact that the maximal number of edges of planar map on n vertices is $3n - 6$ by Euler's formula.

- *C lies in the contractible region of W'*

  All the dual edges of W' are edges of G oriented from its contractible region toward its exterior. Consider the graph G_{out} obtained from G by removing all the edges that are cut by W' and all the vertices and edges that lie in the contractible region of W'. As G is a map, the face of G_{out} containing W' is homeomorphic to an open disk. Let F be its facial walk (in G_{out}) and let k be the length of F. We consider the map obtained from the facial walk F by putting back the vertices and edges that lied inside. We transform this map into a plane map G' by duplicating the vertices and edges appearing several times in F, in order to obtain a triangulation of a cycle of length k. Let n', m', f' be the number of vertices, edges and faces of G'. Every inner vertex of G' has outdegree 3, there are no other inner edges, so the total number of edges of G' is $m' = 3(n' - k) + k$. All the inner faces have length 3 and the outer face has length k, so $2m' = 3(f' - 1) + k$. By Euler's formula $n' - m' + f' = 2$. Combining the three equalities gives $k = 3$ and F is hence a separating triangle of G. This contradicts the choice of the root angle, as it should not lie in the strict interior of a separating triangle.

□

A *Hamiltonian cycle* of a graph is a cycle visiting every vertex once.

Lemma 5 *The cycle C is a Hamiltonian cycle of the angle graph, all the edges of G are marked exactly twice, the subgraph Q of G^* is spanning, and, if $n \geq 2$, the subgraph P of G is spanning.*

Proof Suppose for a contradiction that $\overline{C}$ is non empty. By Lemma 4 and Sect. 4, the frontier T between C and $\overline{C}$ is a union of oriented closed walks of P. Hence a face of G has either all its angles in C or all its angles in $\overline{C}$. Moreover T is a non-empty union of oriented closed walk of P that are oriented clockwise according to the set of faces containing $\overline{C}$ (see the first case of Fig. 11). This set does not contain f_0 since a_0 is in f_0 and C. As in Sect. 3, let $\mathcal{F}$ be the set of counterclockwise facial

walks of G and F_0 be the counterclockwise facial walk of f_0. Let $\mathcal{F}' = \mathcal{F} \setminus F_0$, and $\mathcal{F}_{\overline{C}} \subseteq \mathcal{F}'$ be the set of counterclockwise facial walks of the faces containing $\overline{C}$. We have $\phi(T) = -\sum_{F \in \mathcal{F}_{\overline{C}}} \phi(F)$. So T is a clockwise non-empty 0-homologous oriented subgraph w.r.t. f_0. This contradicts Lemma 1 and the minimality of the orientation w.r.t. f_0. So $\overline{C}$ is empty, thus C is Hamiltonian and all the edges of G are marked twice.

Suppose for a contradiction that $n \geq 2$ and P is not spanning. Since the algorithm starts at v_0, P is not covering a vertex v of G different from v_0. Then the angles around v cannot be visited since by Fig. 11 the only way to move from an angle of one vertex to an angle of another vertex is through an edge of P incident to them. So P is spanning. The proof is similar for Q (note that in this case we have $f \geq 2$). □

Lemma 6 *The first cycle created in P (resp. in Q) by the algorithm is oriented.*

Proof Let e be the first edge creating a cycle in P while executing ALGORITHM PS and consider the steps of ALGORITHM PS before e is added to P. So P is a tree during all these steps. For every vertex of P we define $P(v)$ the unique path from v to v_0 in P (while P is empty at the beginning of the execution, we define $P(v_0) = \{v_0\}$). By Lemma 3, this path $P(v)$ is an oriented path. We prove the following

Claim 1 *Consider a step of the algorithm before e is added to P and where the algorithm is considering a vertex v. Then all the angles around the vertices of P different from the vertices of $P(v)$ are already visited.*

Proof Suppose by contradiction that there is such a step of the algorithm where some angles around the vertices of P different from the vertices of $P(v)$ have not been visited. Consider the first such step. Then clearly we are not at the beginning of the algorithm since $P = P(v) = \{v_0\}$. So at the step just before, the conclusion holds and now it does not hold anymore. Clearly at the step before we were considering a vertex v' distinct from v, otherwise $P(v)$ and P have not changed and we have the conclusion. So from v' to v we are either in Case 1 or Case 4 of ALGORITHM PS (see Fig. 12). If v has been considered by Case 1, then $P(v)$ contains $P(v')$ and the conclusion holds. If v has been considered by Case 4, then since P is a tree, all the angles around v' have been considered and v' is the only element of $P \setminus P(v)$ that is not in $P \setminus P(v')$. Thus the conclusion also holds. □

Consider the iteration of ALGORITHM PS where e is added to P. The edge e is added to P by Case 1, so e is oriented from a vertex u to a vertex v such that v is already in P or v is the root vertex v_0. Consider the step of the algorithm just before u is added to P. By Claim 1, vertex u is not in $P \setminus P(v)$ (otherwise e would have been considered before and it would be a stem). So $u \in P(v)$ and $P(v) \cup \{e\}$ induces an oriented cycle of G. The proof is similar for Q. □

Lemma 7 *P is a spanning unicellular map of G and Q is a spanning tree of G^*. Moreover one is the dual of the complement of the other.*

Proof Suppose that Q contains a cycle, then by Lemma 6 it contains an oriented cycle of G^*. This cycle is contractible by Lemma 2. Recall that by Lemma 5, C is a

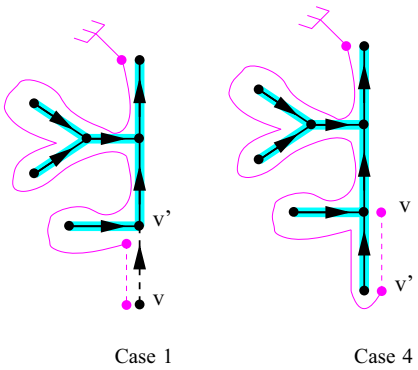

Fig. 12 The two cases of the proof of Claim 1

Hamiltonian cycle, moreover it does not cross Q, a contradiction. So Q contains no cycle and is a tree.

By Lemma 5, all the edges of G are marked at the end. So every edge of G is either in P or its dual in Q (and not both). Thus P and Q are the dual of the complement of each other. So P is the dual of the complement of a spanning tree of G^*. Thus P is a spanning unicellular map of G. □

Theorem 3 is then a direct reformulation of Lemma 7 by the definition of P and Q.

A toroidal unicellular map on n vertices has exactly $n+1$ edges: $n-1$ edges of a tree plus 2 edges corresponding to the size of a basis of the homology (i.e. plus $2g$ in general for an oriented surface of genus g). Thus a consequence of Theorem 3 is that the obtained unicellular map U has exactly n vertices, $n+1$ edges and $2n-1$ stems since the total number of edges is $3n$. The orientation of G induces an orientation of U such that the stems are all outgoing, and such that while walking clockwise around the unique face of U from a_0, the first time an edge is met, it is oriented counterclockwise according to this face, see Fig. 13 where all the tree-like parts and stems are not represented. There are two types of toroidal unicellular maps depicted in Fig. 13. Two cycles of U may intersect either on a single vertex (square case) or on a path (hexagonal case). The square can be seen as a particular case of the hexagon where one side has length zero and thus the two corners of the hexagon are identified.

In Fig. 14, we give several examples of executions of ALGORITHM PS on minimal 3-orientations. These examples show how important is the choice of the minimal HTC Schnyder wood in order to obtain Theorem 3. In particular, the third example shows that ALGORITHM PS can visit all the angles of the triangulation (i.e. the cycle in the angle graph is Hamiltonian) without outputting a unicellular map.

Note that the orientations of Fig. 14 are not Schnyder woods. One may wonder if the fact of being a Schnyder wood is of any help for our method. This is not the case since there are examples of minimal Schnyder woods that are not HTC and where ALGORITHM PS does not visit all the vertices. One can obtain such an example by replicating 3 times horizontally and then 3 times vertically the second example of Fig. 14 to form a 3×3 tiling and starts ALGORITHM PS from the same root angle. Conversely, there are minimal Schnyder woods that are not HTC where ALGORITHM

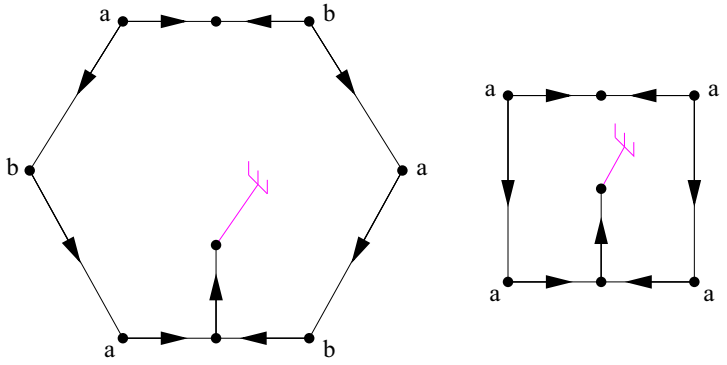

Fig. 13 The two types of rooted toroidal unicellular maps

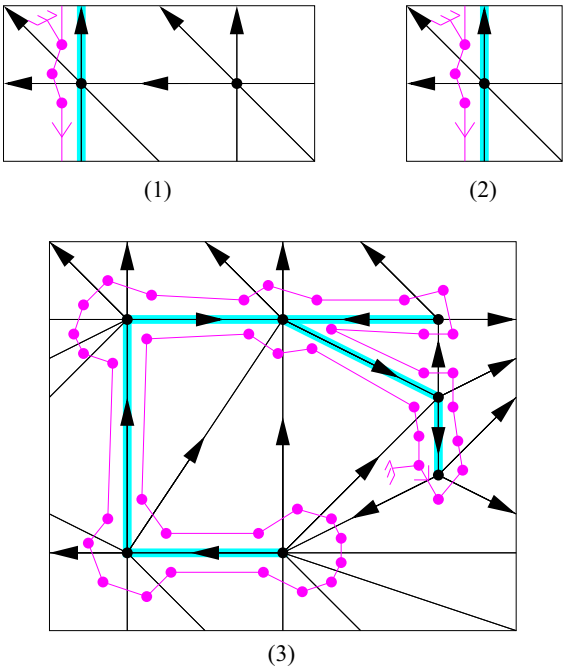

Fig. 14 Examples of minimal 3-orientations that are not HTC Schnyder woods and where ALGORITHM PS respectively: **1** does not visit all the vertices, **2** visits all the vertices but not all the angles, and **3** visits all the angles but does not output an unicellular map

PS does output a toroidal spanning unicellular map (the Schnyder wood of Fig. 7 can serve as an example while starting from an angle of the only face oriented clockwise).

6 Recovering the Original Triangulation

This section is dedicated to show how to recover the original triangulation from the output of ALGORITHM PS. The method is very similar to [20] since like in the plane

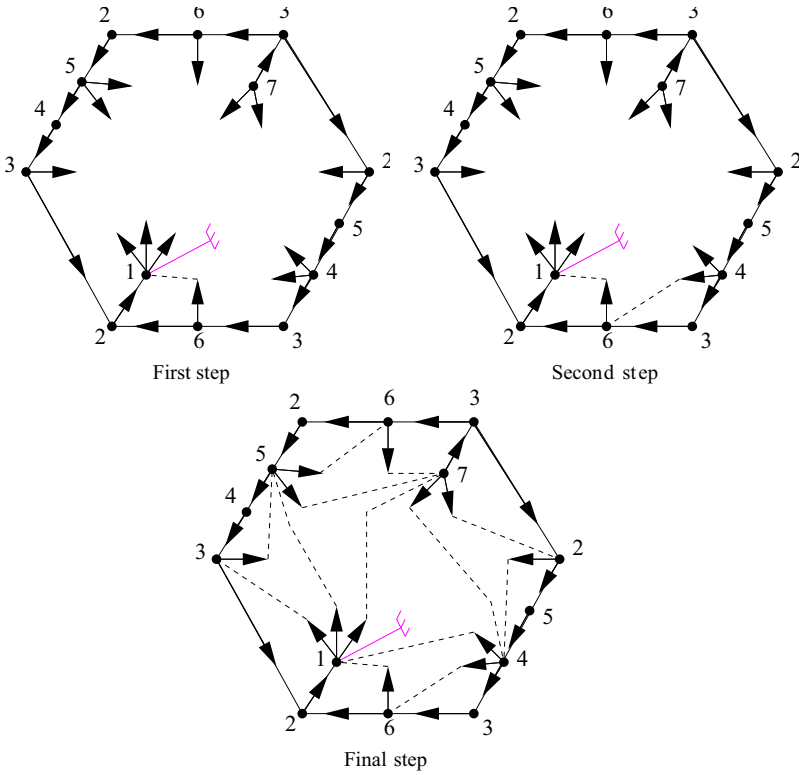

Fig. 15 Example of how to recover the original toroidal triangulation K_7 from the output of ALGORITHM PS

the output has only one face that is homeomorphic to an open disk (i.e. a tree in the plane and a unicellular map in general).

Theorem 4 *Consider a toroidal triangulation G, a root angle a_0 that is not in the strict interior of a separating triangle and the orientation of the edges of G corresponding to the minimal HTC Schnyder wood w.r.t. the root face f_0 containing a_0. From the output U of* ALGORITHM PS *applied on (G, a_0) one can reattach all the stems to obtain G by starting from the root angle a_0 and walking along the face of U in counterclockwise order (according to this face): each time a stem is met, it is reattached in order to create a triangular face on its left side.*

Theorem 4 is illustrated in Fig. 15 where one can check that the obtained toroidal triangulation is K_7 (like on the input of Fig. 9).

In fact in this section we define a method, more general than the one described in Theorem 4, that will be useful in next sections.

Let $\mathcal{U}_r(n)$ denote the set of toroidal unicellular maps U rooted on a particular angle, with exactly n vertices, $n+1$ edges and $2n-1$ stems satisfying the following property. A vertex that is not the root, has exactly 2 stems if it is not a corner, 1 stem if it is the corner of an hexagon and 0 stem if it is the corner of a square. The root vertex

has 1 additional stem, i.e. it has 3 stems if it is not a corner, 2 stems if it is the corner of an hexagon and 1 stem if it is the corner of a square. Note that the output U of ALGORITHM PS given by Theorem 3 is an element of $\mathcal{U}_r(n)$.

Similarly to the planar case [20], we define a general way to reattach step by step all the stems of an element U of $\mathcal{U}_r(n)$. Let $U_0 = U$, and, for $1 \leq k \leq 2n-1$, let U_k be the map obtained from U_{k-1} by reattaching one of its stem (we explicit below which stem is reattached and how). The *special face of* U_0 is its only face. For $1 \leq k \leq 2n-1$, the *special face of* U_k is the face on the right of the stem of U_{k-1} that is reattached to obtain U_k. For $0 \leq k \leq 2n-1$, the border of the special face of U_k consists of a sequence of edges and stems. We define an *admissible triple* as a sequence (e_1, e_2, s), appearing in counterclockwise order along the border of the special face of U_k, such that $e_1 = (u, v)$ and $e_2 = (v, w)$ are edges of U_k and s is a stem attached to w. The *closure* of the admissible triple consists in attaching s to u, so that it creates an edge (w, u) oriented from w to u and so that it creates a triangular face (u, v, w) on its left side. The *complete closure* of U consists in closing a sequence of admissible triple, i.e. for $1 \leq k \leq 2n-1$, the map U_k is obtained from U_{k-1} by closing any admissible triple.

Note that, for $0 \leq k \leq 2n-1$, the special face of U_k contains all the stems of U_k. The closure of a stem reduces the number of edges on the border of the special face and the number of stems by 1. At the beginning, the unicellular map U_0 has $n+1$ edges and $2n-1$ stems. So along the border of its special face, there are $2n+2$ edges and $2n-1$ stems. Thus there is exactly three more edges than stems on the border of the special face of U_0 and this is preserved while closing stems. So at each step there is necessarily at least one admissible triple and the sequence U_k is well defined. Since the difference of three is preserved, the special face of U_{2n-2} is a quadrangle with exactly one stem. So the reattachment of the last stem creates two faces that have length three and at the end U_{2n-1} is a toroidal triangulation. Note that at a given step there might be several admissible triples but their closure are independent and the order in which they are performed does not modify the obtained triangulation U_{2n-1}.

We now apply the closure method to our particular case. Consider a toroidal triangulation G, a root angle a_0 that is not in the strict interior of a separating triangle and the orientation of the edges of G corresponding to the minimal HTC Schnyder wood w.r.t. the root face f_0. Let U be the output of ALGORITHM PS applied on (G, a_0).

Lemma 8 *When a stem of U is reattached to form the corresponding edge of G, it splits the (only) face of U into two faces. The root angle of U is in the face that is on the right side of the stem.*

Proof By Lemma 5, the execution of ALGORITHM PS corresponds to a Hamiltonian cycle $C = (a_0, \ldots, a_{2m}, a_0)$ in the angle graph of G. Thus C defines a total order $<$ on the angles of G where $a_i < a_j$ if and only if $i < j$. Let us consider now the angles on the face of U. Note that such an angle corresponds to several angles of G, that are consecutive in C and that are separated by a set of incoming edges of G (those incoming edges corresponding to stems of U). Thus the order on the angles of G defines automatically an order on the angles of U. The angles of U considered in clockwise order along the border of its face, starting from the root angle, correspond to a sequence of strictly increasing angles for $<$.

Consider a stem s of U that is reattached to form an edge e of G. Let a_s be the angle of U that is situated just before s (in clockwise order along the border of the face of U) and a'_s be the angle of U where s should be reattached. If $a'_s < a_s$, then when ALGORITHM PS consider the angle a_s, the edge corresponding to s is already marked and we are not in Case 2 of ALGORITHM PS . So $a_s < a'_s$ and a_0 is on the right side of s. □

Recall that U is an element of $\mathcal{U}_r(n)$ so we can apply on U the complete closure procedure described above. We use the same notation as before, i.e. let $U_0 = U$ and for $1 \leq k \leq 2n-1$, the map U_k is obtained from U_{k-1} by closing any admissible triple. The following lemma shows that the triangulation obtained by this method is G:

Lemma 9 *The complete closure of U is G, i.e. $U_{2n-1} = G$.*

Proof We prove by induction on k that every face of U_k is a face of G, except for the special face. This is true for $k = 0$ since $U_0 = U$ has only one face, the special face. Let $0 \leq k \leq 2n-2$, and suppose by induction that every non-special face of U_k is a face of G. Let (e_1, e_2, s) be the admissible triple of U_k such that its closure leads to U_{k+1}, with $e_1 = (u, v)$ and $e_2 = (v, w)$. The closure of this triple leads to a triangular face (u, v, w) of U_{k+1}. This face is the only "new" non-special face while going from U_k to U_{k+1}.

Suppose, by contradiction, that this face (u, v, w) is not a face of G. Let a_v (resp. a_w) be the angle of U_k at the special face, between e_1 and e_2 (resp. e_2 and s). Since G is a triangulation, and (u, v, w) is not a face of G, there exists at least one stem of U_k that should be attached to a_v or a_w to form a proper edge of G. Let s' be such a stem that is the nearest from s. In G the edges corresponding so s and s' should be incident to the same triangular face. Let x be the origin of the stem s'. Let $z \in \{v, w\}$ such that s' should be reattached to z. If $z = v$, then s should be reattached to x to form a triangular face of G. If $z = w$, then s should be reattached to a common neighbor of w and x located on the border of the special face of U_k in counterclockwise order between w and x. So in both cases s should be reattached to a vertex y located on the border of the special face of U_k in counterclockwise order between w and x (with possibly $y = x$). To summarize s goes from w to y and s' from x to z, and z, x, y, w appear in clockwise order along the special face of U_k. By Lemma 8, the root angle is on the right side of both s and s', this is not possible since their right sides are disjoint, a contradiction.

So for $0 \leq k \leq 2n-2$, all the non-special faces of U_k are faces of G. In particular every face of U_{2n-1} except one is a face of G. Then clearly the (triangular) special face of U_{2n-1} is also a face of G, hence $U_{2n-1} = G$. □

Lemma 9 shows that one can recover the original triangulation from U with any sequence of admissible triples that are closed successively. This does not explain how to find the admissible triples efficiently. In fact the root angle can be used to find a particular admissible triple of U_k:

Lemma 10 *For $0 \leq k \leq 2n-2$, let s be the first stem met while walking counterclockwise from a_0 in the special face of U_k. Then before s, at least two edges are met and the last two of these edges form an admissible triple with s.*

Proof Since s is the first stem met, there are only edges that are met before s. Suppose by contradiction that there is only zero or one edge met before s. Then the reattachment of s to form the corresponding edge of G is necessarily such that the root angle is on the left side of s, a contradiction to Lemma 8. So at least two edges are met before s and the last two of these edges form an admissible triple with s. □

Lemma 10 shows that one can reattach all the stems by walking once along the face of U in counterclockwise order. Thus we obtain Theorem 4.

Note that U is such that the complete closure procedure described here never *wraps over the root angle*, i.e. when a stem is reattached, the root angle is always on its right side (see Lemma 8). The property of never wrapping over the root angle is called *balanced* in [2]. Let $\mathcal{U}_{r,b}(n)$ denote the set of elements of $\mathcal{U}_r(n)$ that are balanced. So the output U of ALGORITHM PS given by Theorem 3 is an element of $\mathcal{U}_{r,b}(n)$. We exhibit in Sect. 9 a bijection between appropriately rooted toroidal triangulations and a particular subset of $\mathcal{U}_{r,b}(n)$.

The possibility to close admissible triples in any order to recover the original triangulation is interesting compared to the simpler method of Theorem 4 since it enables to recover the triangulation even if the root angle is not given. This property is used in Sect. 11 to obtain a bijection between toroidal triangulations and some unrooted unicellular maps.

Moreover if the root angle is not given, then one can simply start from any angle of U, walk twice around the face of U in counterclockwise order and reattach all the admissible triples that are encountered along this walk. Walking twice ensures that at least one complete round is done from the root angle. Since only admissible triples are considered, we are sure that no unwanted reattachment is done during the process and that the final map is G. This enables to reconstruct G in linear time even if the root angle is not known. This property is used in Sect. 7.

7 Optimal Encoding

The results presented in the previous sections allow us to generalize the encoding of planar triangulations, defined by Poulalhon and Schaeffer [20], to triangulations of the torus. The construction is direct and it is hence really different from the one of [3] where triangulations of surfaces are cut in order to deal with planar triangulations with boundaries. Here we encode the unicellular map outputted by ALGORITHM PS by a plane rooted tree with n vertices and with exactly two stems attached to each vertex, plus $O(\log(n))$ bits. As in [3], this encoding is asymptotically optimal and uses approximately $3.2451n$ bits. The advantage of our method is that it can be implemented in linear time. Moreover we believe that our encoding gives a better understanding of the structure of triangulations of the torus. It is illustrated with new bijections that are obtained in Sects. 9 and 11 .

Consider a toroidal triangulation G, a root angle a_0 that is not in the strict interior of a separating triangle and the orientation of the edges of G corresponding to the minimal HTC Schnyder wood w.r.t. the root face f_0. Let U be the output of ALGORITHM PS applied on (G, a_0). As already mentioned at the end of Sect. 6, to retrieve the triangulation G one just needs to know U without the information of its root angle

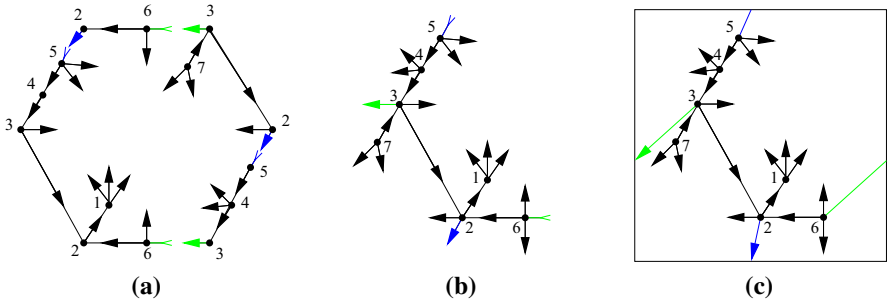

Fig. 16 From unicellular maps to trees with special stems and back

(by walking twice around the face of U in counterclockwise order and reattaching all the admissible triples that are encountered along this walk, one can recover G). Hence to encode G, one just has to encode U without the position of the root angle around the root vertex (see Fig. 16a).

By Lemma 3, the unicellular map U contains a spanning tree T which is oriented from the leaves to the root vertex. The tree T contains exactly $n-1$ edges, so there is exactly 2 edges of U that are not in T. We call these edges the *special edges* of U. We cut these two special edges to transform them into stems of T (see Fig. 16a, b). We keep the information of where are the special stems in T and on which angle of T they should be reattached. This information can be stored with $O(\log(n))$ bits. One can recover U from T by reattaching the special stems in order to form non-contractible cycles with T (see Fig. 16c).

So T is a plane tree on n vertices, each vertex having 2 stems except the root vertex v_0 having three stems. Choose any stem s_0 of the root vertex, remove it and consider that T is rooted at the angle where s_0 should be attached. The information of the root enables to put back s_0 at its place. So now we are left with a rooted plane tree T on n vertices where each vertex has exactly 2 stems (see Fig. 17a).

This tree T can easily be encoded by a binary word on $6n-2$ bits: that is, walking in counterclockwise order around T from the root angle, writing a "1" when going down along T (our convention for *down* is with the root vertex at the top), and a "0" when going up along T (see Fig. 17a). As in [20], one can encode T more compactly by using the fact that each vertex has exactly two stems. Thus T is encoded by a binary word on $4n-2$ bits: that is, walking in counterclockwise order around T from the root angle, writing a "1" when going down along an edge of T, and a "0" when going up along an edge or along a stem of T (see Fig. 17b where the "red 1's" of Fig. 17a have been removed). Indeed there is no need to encode when going down along stems, as this information can be retrieved afterward. While reading the binary word to recover T, when a "0" is met, we should go up in the tree, except if the vertex that we are considering does not have already its two stems, then in that case we should create a stem (i.e. add a "red 1" before the "0"). So we are left with a binary word on $4n-2$ bits with exactly $n-1$ bits "1" and $3n-1$ bits "0".

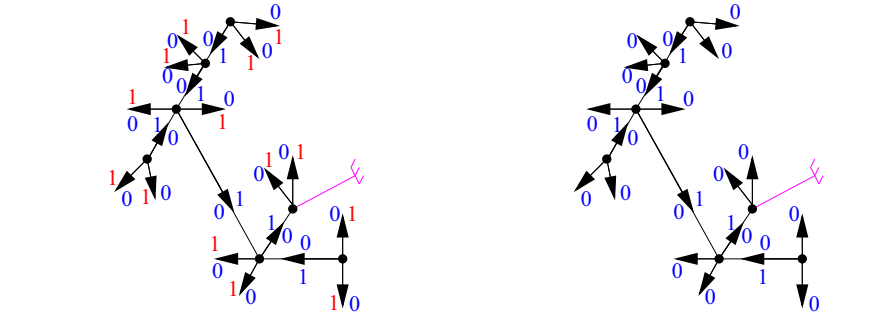

Fig. 17 Encoding a rooted tree with two stems at each vertex

Similarly to [20], using [6, Lem. 7], this word can then be encoded with a binary word of length $\log_2 \binom{4n-2}{n-1} + o(n) \sim n \log_2 \left(\frac{256}{27}\right) \approx 3.2451\, n$ bits. Thus we have the following theorem whose linearity is discussed in Sect. 8:

Theorem 5 *Any toroidal triangulation on n vertices, can be encoded with a binary word of length* $3.2451n + o(n)$ *bits, the encoding and decoding being linear in n.*

8 Linear Complexity

In this section we show that the encoding method described in this paper, that is encoding a toroidal triangulation via a unicellular map and recovering the original triangulation, can be performed in linear time. The only difficulty lies in providing ALGORITHM PS with the appropriate input it needs in order to apply Theorem 3. Then clearly the execution of ALGORITHM PS, the encoding phase and the recovering of the triangulation are linear. Thus we have to show how one can find in linear time a root angle a_0 that is not in the strict interior of a separating triangle, as well as the minimal HTC Schnyder wood w.r.t. the root face f_0.

Consider a toroidal triangulation G. Let us see how one can build a Schnyder wood of G in linear time. The *contraction* of a non-loop-edge e of G is the operation consisting of continuously contracting e until merging its two ends, as shown in Fig. 18. Note that only one edge of each pair of homotopic multiple edges is preserved (edges e_{wx} and e_{wy} in the figure). Note that the contraction operation is also defined when some vertices are identified: $x = u$ and $y = v$, or, $x = v$ and $y = u$.

An edge e is said to be *contractible* if it is not a loop and if after contracting e and identifying the borders of the two newly created length two faces, one obtains a triangulation that is still without contractible loop or homotopic multiple edges. In [15] the existence of crossing Schnyder wood is proved by contraction. Unfortunately this proof cannot easily be transformed into a linear algorithm because of the crossing property that has to be maintained during the contraction process. Nevertheless we use contractions to obtain non-necessarily crossing Schnyder woods. If the triangulation

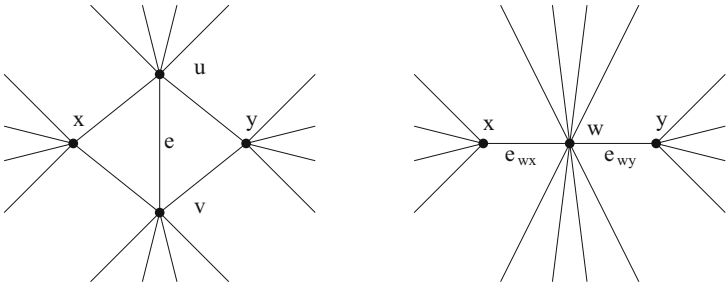

Fig. 18 The contraction operation

obtained after contracting a contractible edge admits a Schnyder wood it is then easy to obtain a Schnyder wood of G. The rules for decontracting an edge in the case of toroidal triangulations are depicted in [15, Fig. 21] where for each case one can choose any of the proposed colorings. For any toroidal triangulation, one can find contractible edges until the toroidal map has only one vertex (see [19]). A Schnyder wood of the toroidal map on one vertex is depicted on the right of Fig. 3. Thus one can obtain a Schnyder wood of any toroidal triangulation by this process. Nevertheless, to maintain linearity we have to be more precise since it is not trivial to find contractible edges.

Consider an edge e of G with distinct ends u, v, and with incident faces uvx and vuy, such that these vertices appear in clockwise order around the corresponding face (so we are in the situation of Figure 18). The edge e is contractible if and only if, every walk enclosing an open disk containing a face other than uvx and vuy, goes through an edge distinct from e at least three times. Equivalently e is non-contractible if and only if it belongs to a separating triangle or u, v are both incident to a loop-edge ℓ_u, ℓ_v, respectively, such that the walk of length four (ℓ_u, e, ℓ_v, e) encloses an open disk with at least three faces (i.e. with at least one face distinct from uvx and vuy). To avoid the latter case, if vertex u is incident to a loop-edge ℓ_u, we consider e to be an edge that is consecutive to that loop, so that we have $x = u$. In such a case, if there is a loop ℓ_v incident to v and a walk of length four of the form (ℓ_u, e, ℓ_v, e) enclosing a disk with at least three faces, then there is also a separating triangle containing e. In the following we show how to find such separating triangle, if there is one. If u and v have more common neighbors, than simply x and y, consider their second common neighbor going clockwise around u from e (the first one being x, and the last being y) and call it x'. Call y' their second common neighbor going counterclockwise around u from e. Now, either uvx' or uvy' is a separating triangle or the edge e is contractible. We consider these two cases below:

- If e is contractible, then it is contracted and we apply the procedure recursively to obtain a Schnyder wood of the contracted graph. Then we update the Schnyder wood as described above. Note that this update is done in constant time.
- If uvx' (resp. uvy') is a separating triangle, one can remove its interior, recursively obtain a toroidal Schnyder wood of the remaining toroidal triangulation, build a planar Schnyder wood of the planar triangulation inside uvx' (resp. uvy'), and then superimpose the two (by eventually permuting the colors) to obtain a Schnyder

wood of the whole graph. Note that computing a planar Schnyder wood can be done in linear time using a canonical ordering (see [17]).

The difficulty here is to test whether uvx' or uvy' are triangles. For that purpose, one first needs to compute a basis (B_1, B_2) for the homology. Consider a spanning tree of the dual map G^*. The map obtained from G by removing those edges is unicellular, and removing its treelike parts one obtains two cycles (B_1, B_2) (intersecting on a path with at least one vertex) that form a basis for the homology. This can be computed in linear time for G and then updated when some edge is contracted or when the interior of some separating triangle is removed. The updating takes constant time when some edge is contracted, and it takes $O(n')$ time when removing n' vertices in the interior of some separating triangle. The overall cost of constructing and maintaining the basis is thus linear in the size of G. Then a closed walk of length three W, given with an arbitrary orientation, encloses a region homeomorphic to an open disk if and only if W crosses B_i from right to left as many times as W crosses B_i from left to right, for every $i \in \{1, 2\}$. This test can be done in constant time for uvx' and uvy' once the half edges on the right and left sides of the cycles B_i are marked. Marking the half edges of G and maintaining this marking while contracting edges or while removing the interior of separating triangles can clearly be done in linear time. We thus have that the total running time to compute a Schnyder wood of G is linear.

From this Schnyder wood, one can compute in linear time a root angle a_0 not in the strict interior of a separating triangle. First note that in a 3-orientation of a toroidal triangulation, the edges that are inside a separating triangle and that are incident to the three vertices on the border are all oriented toward these three vertices by Euler's formula. Thus an oriented non-contractible cycle cannot enter in the interior of a separating triangle. Now follow any oriented monochromatic path of the Schnyder wood and stop the first time this path is back to a previously met vertex v_0. The end of this path forms an oriented monochromatic cycle C containing v_0. If C is a contractible cycle then Euler's formula is violated in the contractible region. Thus C is an oriented non-contractible cycle and cannot contain some vertices that are in the interior of a separating triangle. So v_0 is not in the interior of a separating triangle and we can choose as root angle a_0 any angle incident to v_0.

In [16] (see also [18]) it is proved how one can transform any 3-orientation (hence a Schnyder wood) of a toroidal triangulation into a HTC Schnyder wood. The method consists in computing a so called "middle-path" (a directed path where the next edge chosen is the one leaving in the "middle") and reversing some non-contractible "middle-cycles". Clearly the method is linear even if not explicitly mentioned in [16]. Let D_0 be the corresponding obtained orientation of G.

It remains to compute the minimal HTC Schnyder wood w.r.t. the root face f_0. There is a generic known method Meunier, F.: Personal communication (2015) (see also [23, p. 23]) to compute in linear time a minimal α-orientation of a planar map as soon as an α-orientation is given. This method also works on oriented surfaces and can be applied to obtain the minimal HTC Schnyder wood in linear time. We explain the method briefly below.

It is much simpler to compute the minimal orientation $D_{\min}$ homologous to D_0 in a dual setting. The first observation to make is that two orientations D_1, D_2 of G

are homologous if and only if there dual orientations D_1^*, D_2^* of G^* are equivalent up to reversing some directed cuts. Furthermore $D_1 \preceq_{f_0} D_2$ if and only if D_1^* can be obtained from D_2^* by reversing directed cuts oriented from the part containing f_0. Let us compute $D^*_{\min}$ which is the only orientation of G^*, obtained from D_0^* by reversing directed cuts, and without any directed cut oriented from the part containing f_0. For this, consider the orientation D_0^* of $G^* = (F, E^*)$ and compute the set $X \subseteq F$ of vertices of G^* that have an oriented path toward f_0. Then $(X, F \setminus X)$ is a directed cut oriented from the part containing f_0 that one can reverse. Then update the set of vertices that can reach f_0 and go on until $X = F$. It is not difficult to see that this can be done in linear time. Thus we obtain the minimal HTC Schnyder wood w.r.t. f_0 in linear time.

9 Bijection with Rooted Unicellular Maps

Given a toroidal triangulation G with a root angle a_0, we have defined a unique associated orientation: the minimal HTC Schnyder wood w.r.t. the root face f_0. Suppose that G is oriented according to the minimal HTC Schnyder wood. If a_0 is not in the strict interior of a separating triangle then Theorems 3 and 4 show that the execution of ALGORITHM PS on (G, a_0) gives a toroidal unicellular map with stems from which one can recover the original triangulation. Thus there is a bijection between toroidal triangulations rooted from an appropriate angle and their image by ALGORITHM PS. The goal of this section is to describe this image.

Recall from Sect. 6 that the output of ALGORITHM PS on (G, a_0) is an element of $\mathcal{U}_{r,b}(n)$. One may hope that there is a bijection between toroidal triangulations rooted from an appropriate angle and $\mathcal{U}_{r,b}(n)$ since this is how it works in the planar case. Indeed, given a planar triangulation G, there is a unique orientation of G (the minimal Schnyder wood) on which ALGORITHM PS, performed from an outer angle, outputs a spanning tree. In the toroidal case, things are more complicated since the behavior of ALGORITHM PS on minimal HTC Schnyder woods does not characterize such orientations.

Figure 19 gives an example of two (non-homologous) orientations of the same triangulation that are both minimal w.r.t. the same root face. For these two orientations, the execution of ALGORITHM PS from the same root angle gives two different elements of $\mathcal{U}_{r,b}(2)$ (from which the original triangulation can be recovered by the method of Theorem 4). Thus we have to exhibit a particular property of HTC Schnyder woods that can be used to characterize which particular subset of $\mathcal{U}_{r,b}(n)$ is in bijection with appropriately rooted toroidal triangulations.

For that purpose we now introduce a function γ which is reminiscent to the one in [16]. Consider a particular orientation of G. Let C be a cycle that is given with an arbitrary direction (C is not necessarily a directed cycle). Then $\gamma(C)$ is defined by,

$$\gamma(C) = \#\text{ edges leaving } C \text{ on its right } - \#\text{ edges leaving } C \text{ on its left}.$$

By the Schnyder property, it is clear that in a toroidal Schnyder wood, a monochromatic cycle C always satisfies $\gamma(C) = 0$. Consider a crossing Schnyder wood

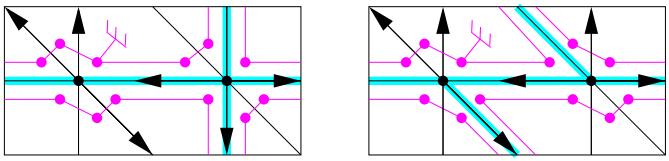

Fig. 19 A graph that can be represented by two different unicellular maps

of G and C_1, C_2 two monochromatic cycles of different colors. Thus we have $\gamma(C_1) = \gamma(C_2) = 0$. By [15, Thm. 7], the two cycles C_1, C_2 are non-contractible and non-homologous, thus they form a basis for the homology. While returning a 0-homologous oriented subgraph, the value of γ on a given cycle does not change. Thus any HTC Schnyder wood also satisfies $\gamma(C_1) = \gamma(C_2) = 0$. Moreover it is proved in [16] (see also [18]) that if a 3-orientation of a toroidal triangulation satisfies γ equals 0 for two cycles forming a basis for the homology, then γ equals 0 for any non-contractible cycle. Thus any HTC Schnyder wood satisfies γ equals 0 for any non-contractible cycle. We call this property the γ_0 *property*. Note that, for a 3-orientation, it is sufficient to satisfy γ equals 0 on any two cycles forming a basis for the homology to have the γ_0 property.

Actually the γ_0 property characterizes the 3-orientations that are HTC Schnyder woods. Indeed a consequence of [16, Thm. 5 and Lem. 18] is that if two 3-orientations both satisfy the γ_0 property, then they are homologous to each other and thus HTC. Note that for the 3-orientation on the right of Fig. 19, we have γ equals ± 2 for the horizontal cycle and this explain why this orientation is not HTC (one can find similar arguments for previous examples of non-HTC Schnyder woods presented in this paper, see Figs. 5, 7).

Let us translate this γ_0 property on $\mathcal{U}_r(n)$. Consider an element U of $\mathcal{U}_r(n)$ whose edges and stems are oriented w.r.t. the root angle as follows: the stems are all outgoing, and while walking clockwise around the unique face of U from a_0, the first time an edge is met, it is oriented counterclockwise w.r.t. the face of U. Then one can compute γ on the cycles of U (edges and stems count). We say that a unicellular map of $\mathcal{U}_r(n)$ satisfies the γ_0 property if γ equals zero on its (non-contractible) cycles. Let us call $\mathcal{U}_{r,b,\gamma_0}(n)$ the set of elements of $\mathcal{U}_{r,b}(n)$ satisfying the γ_0 property. So the output of ALGORITHM PS given by Theorem 3 is an element of $\mathcal{U}_{r,b,\gamma_0}(n)$.

Let $\mathcal{T}_r(n)$ be the set of toroidal triangulations on n vertices rooted at an angle that is not in the strict interior of a separating triangle. Then we have the following bijection:

Theorem 6 *There is a bijection between* $\mathcal{T}_r(n)$ *and* $\mathcal{U}_{r,b,\gamma_0}(n)$.

Proof Consider the mapping g that associates to an element of $\mathcal{T}_r(n)$, the output of ALGORITHM PS executed on the minimal HTC Schnyder wood w.r.t. the root face. By the above discussion the image of g is in $\mathcal{U}_{r,b,\gamma_0}(n)$ and g is injective since one can recover the original triangulation from its image by Theorem 4.

Conversely, given an element U of $\mathcal{U}_{r,b,\gamma_0}(n)$ with root angle a_0, one can build a toroidal map G by the complete closure procedure described in Sect. 6. The number of stems and edges of U implies that G is a triangulation. Recall that a_0 defines an

orientation on the edges and stems of U. Consider the orientation D of G induced by this orientation. Since U is balanced, the execution of ALGORITHM PS on (G, a_0) corresponds to the cycle in the angle graph of U obtained by starting from the root angle and walking clockwise in the face of U. Thus the output of ALGORITHM PS executed on (G, a_0) is U. It remains to show that G is appropriately rooted and that D corresponds to the minimal HTC Schnyder wood w.r.t. this root.

First note that by definition of $\mathcal{U}_r(n)$, the orientation D is a 3-orientation.

Suppose by contradiction that a_0 is in the strict interior of a separating triangle. Then, since we are considering a 3-orientation, by Euler's formula, the edges in the interior of this triangle and incident to its border are all entering the border. So ALGORITHM PS started from the strict interior cannot visit the vertices on the border of the triangle and outside. Thus the output of ALGORITHM PS is not a toroidal unicellular map, a contradiction. So a_0 is not in the strict interior of a separating triangle.

The γ_0 property of U implies that γ equals zero on two cycles of U. Hence these two cycles considered in G also satisfy γ equals 0 and form a basis for the homology. So D is an HTC Schnyder wood.

Suppose by contradiction that D is not minimal. Then, by Lemma 1, it contains a clockwise (non-empty) 0-homologous oriented subgraph w.r.t. f_0. With the notations of Sect. 3, let T be such a subgraph with $\phi(T) = -\sum_{F \in \mathcal{F}'} \lambda_F \phi(F)$, with $\lambda \in \mathbb{N}^{|\mathcal{F}'|}$. Let $\lambda_{F_0} = 0$, and $\lambda_{\max} = \max_{F \in \mathcal{F}} \lambda_F$. For $0 \leq i \leq \lambda_{\max}$, let $X_i = \{F \in \mathcal{F} \mid \lambda_F \geq i\}$. For $1 \leq i \leq \lambda_{\max}$, let T_i be the oriented subgraph such that $\phi(T_i) = -\sum_{F \in X_i} \phi(F)$. Then we have $\phi(T) = \sum_{1 \leq i \leq \lambda_{\max}} \phi(T_i)$. Since T is an oriented subgraph, we have $\phi(T) \in \{-1, 0, 1\}^{|E(G)|}$. Thus for any edge of G, incident to faces F_1 and F_2, we have $(\lambda_{F_1} - \lambda_{F_2}) \in \{-1, 0, 1\}$. So, for $1 \leq i \leq \lambda_{\max}$, the oriented graph T_i is the frontier between the faces with λ value equal to i and $i - 1$. So all the T_i are edge disjoint and are oriented subgraphs of D. Since T is non-empty, we have $\lambda_{\max} \geq 1$, and T_1 is non-empty. All the edges of T_1 have a face of X_1 on their right and a face of X_0 on their left. Since U is an unicellular map, and T_1 is a (non-empty) 0-homologous oriented subgraph, at least one edge of T_1 corresponds to a stem of U. Let s be the last stem of U corresponding to a edge of T_1 that is reattached by the complete closure procedure. Consider the step where s is reattached. As the root angle (and thus f_0) is in the special face (see the terminology of Sect. 6), the special face is in the region defined by X_0. Thus it is on the left of s when it is reattached. This contradicts the fact that U is balanced. Thus D is the minimal HTC Schnyder wood w.r.t. f_0. □

10 The Lattice of HTC Schnyder Woods

In this section, we push further the study of HTC Schnyder woods in order to remove the root and the balanced property of the unicellular maps considered in Theorem 6 and obtain a simplified bijection in Theorem 7 of Sect. 11.

Consider a toroidal triangulation G given with a crossing Schnyder wood. Let D_0 be the corresponding 3-orientation of G. Let f_0 be any face of G. Recall from Sect. 3 that $O(G)$ denotes the set of all the orientations of G that are homologous to D_0. The elements of $O(G)$ are the HTC Schnyder woods of G and $(O(G), \leq_{f_0})$ is a distributive

lattice. We first recall some general results and terminology from [16] before studying the consequences of considering HTC Schnyder woods.

We need to reduce the graph G. We call an edge of G *rigid* w.r.t. $O(G)$ if it has the same orientation in all the elements of $O(G)$. Rigid edges do not play a role for the structure of $O(G)$. We delete them from G and call the obtained embedded graph $\widetilde{G}$. Note that this graph is embedded but it is not necessarily a map, as some faces may not be homeomorphic to open disks. Note also that $\widetilde{G}$ might be empty if all the edges are rigid, i.e. $|O(G)| = 1$ and $\widetilde{G}$ has no edge but a unique face that is all the surface.

Lemma 11 [16] *Given an edge e of G, the following are equivalent*:

1. *e is non-rigid*,
2. *e is contained in a 0-homologous oriented subgraph of D_0,*
3. *e is contained in a 0-homologous oriented subgraph of any element of $O(G)$.*

By Lemma 11, one can build $\widetilde{G}$ by keeping only the edges that are contained in a 0-homologous oriented subgraph of D_0. Note that this implies that all the edges of $\widetilde{G}$ are incident to two distinct faces of $\widetilde{G}$. Denote by $\widetilde{\mathcal{F}}$ the set of oriented subgraphs of $\widetilde{G}$ corresponding to the boundaries of faces of $\widetilde{G}$ considered counterclockwise. Let $\widetilde{f_0}$ be the face of $\widetilde{G}$ containing f_0 and $\widetilde{F_0}$ be the element of $\widetilde{\mathcal{F}}$ corresponding to the boundary of $\widetilde{f_0}$. Let $\widetilde{\mathcal{F}}' = \widetilde{\mathcal{F}} \setminus \widetilde{F_0}$. The elements of $\widetilde{\mathcal{F}}'$ are sufficient to generate the entire lattice $(O(G), \leq_{f_0})$ (see [16]), i.e. two elements D, D' of $O(G)$ are linked in the Hasse diagram of the lattice, with $D \leq_{f_0} D'$, if and only if $D \setminus D' \in \widetilde{\mathcal{F}}'$.

Lemma 12 [16] *For every element $\widetilde{F} \in \widetilde{\mathcal{F}}$ there exists D in $O(G)$ such that $\widetilde{F}$ is an oriented subgraph of D.*

By Lemma 12, for every element $\widetilde{F} \in \widetilde{\mathcal{F}}'$ there exists D in $O(G)$ such that $\widetilde{F}$ is an oriented subgraph of D. Thus there exists D' such that $\widetilde{F} = D \setminus D'$ and D, D' are linked in the Hasse diagram of the lattice. Thus the elements of $\widetilde{\mathcal{F}}'$ form a minimal set that generates the lattice.

Let $D_{\max}$ (resp. $D_{\min}$) be the maximal (resp. minimal) element of $(O(G), \leq_{f_0})$.

Lemma 13 [16] $\widetilde{F_0}$ (resp. $-\widetilde{F_0}$) is an oriented subgraph of $D_{\max}$ (resp. $D_{\min}$).

From now on we use some specific properties of the object considered in this paper, i.e. HTC Schnyder woods.

Lemma 14 *Consider an orientation D in $O(G)$ and a closed walk W of $\widetilde{G}$. If on the left side of W, there is no incident outgoing edges of D, then W is a triangle with its interior on its left side.*

Proof Consider a closed walk W of $\widetilde{G}$ such that on its left side there is no incident outgoing edges of D. Let W_{left} be the edges of D that are incident to the left side of W. By assumption they are all entering W. Note that W cannot cross itself otherwise it has at least one incident outgoing edges of D on its left side. However it may have repeated vertices but in that case it intersects itself tangentially on the right side.

Suppose first that W is a non-contractible cycle. Then consider the closed walk W^* of the dual orientation D^* that is obtained by considering all the dual edges of

W_{left} with their corresponding orientation. Since all the edges of W_{left} are entering W we have that W^* is an oriented closed walk. Moreover it is non-contractible and thus contains an oriented non-contractible cycle, a contradiction to Lemma 2. So W is not a non-contractible cycle.

Suppose by contradiction that there is an oriented subwalk W' of W, that forms a cycle C enclosing a region R on its right side that is homeomorphic to an open disk. Let v be the starting and ending vertex of W'. Note that we do not consider that W' is a strict subwalk of W, so we might have $W' = W$. Consider the graph G' obtained from G by keeping all the vertices and edges that lie in the region R, including W'. Since W can intersect itself only tangentially on the right side, we have that G' is a plane map whose outer face boundary is W' and whose interior is triangulated. Let k be the length of W'. Let n', m', f' be the number of vertices, edges and faces of G'. By Euler's formula, $n' - m' + f' = 2$. All the inner faces have length 3 and the outer face has length k, so $2m' = 3(f' - 1) + k$. Since there is no outgoing incident edges of D on the left side of W, all the vertices of G', except v, have their outgoing edges in G'. Since W' is oriented, v has at least one outgoing edge in G'. Thus, as we are considering a 3-orientation, we have $m' \geq 3(n' - 1) + 1$. Combining these three equalities gives $k \leq -1$, a contradiction. So there is no oriented subwalk of W, that forms a cycle enclosing an open disk on its right side.

Recall that since there is no incident outgoing edges of G on the left side of W, the walk W can only intersect itself tangentially and on its right side. Thus following W on its left, one draws a curve that does not intersect itself. This curve is thus either enclosing a region homeomorphic to an open disk or forming a non-contractible non-self intersecting curve. Suppose, by contradiction, that we are in the second case. Since there is no subwalk of W, that forms a cycle enclosing an open disk on its right side, we have that W is a non-contractible cycle, a contradiction. So the left side of W encloses a region R homeomorphic to an open disk.

Consider the graph G' obtained from G by keeping only the vertices and edges that lie in the region R, including W. The vertices of W appearing several times are duplicated so that G' is a plane triangulation of a cycle. Let k be the length of W. Let n', m', f' be the number of vertices, edges and faces of G'. By Euler's formula, $n' - m' + f' = 2$. All the inner faces have length 3 and the outer face has length k, so $2m' = 3(f' - 1) + k$. All the inner vertices have outdegree 3 as we are considering a 3-orientation of G. All the edges of W_{left} are oriented toward W, and there are k outer edges, so $m' = 3(n' - k) + k$. Combining these three equalities gives $k = 3$, i.e. W has length three and the lemma holds. □

The boundary of a face of $\widetilde{G}$ may be composed of several closed walks. Let us call *quasi-contractible* the faces of $\widetilde{G}$ that are homeomorphic to a disk or to a disk with punctures. Note that such a face may have several boundaries (if there is some punctures) but exactly one of these boundaries enclose the face. Let us call *outer facial walk* this special boundary. Then we have the following:

Lemma 15 *All the faces of $\widetilde{G}$ are quasi-contractible and their outer facial walk is a triangle.*

Proof Suppose by contradiction that there is a face $\widetilde{f}$ of $\widetilde{G}$ that is not quasi-contractible or whose outer facial walk is not a triangle. Let $\widetilde{F}$ be the element of $\widetilde{\mathcal{F}}$ corresponding to the boundary of $\widetilde{f}$. By Lemma 12, there exists an orientation D in $O(G)$ such that $\widetilde{F}$ is an oriented subgraph of D.

All the faces of G have length three. Thus $\widetilde{f}$ is not a face of G and contains in its interior at least one edge of G. Start from any such edge e and consider the *left-walk* $W = (e_i)_{i\geq 0}$ of D obtained by the following: if the edge e_i is entering a vertex v, then e_{i+1} is choosen among the three edges leaving v as the edge that is on the left coming from e_i (i.e. the first one while going clockwise around v). Suppose that for $i \geq 0$, edge e_i is entering a vertex v that is on the border of $\widetilde{f}$. Recall that by definition $\widetilde{F}$ is oriented counterclockwise according to its interior, so either e_{i+1} is in the interior of $\widetilde{f}$ or e_{i+1} is on the border of $\widetilde{f}$. Thus W cannot leave $\widetilde{f}$.

Since G has a finite number of edges, some edges are used several times in W. Consider a minimal subsequence $W' = e_k, \ldots, e_\ell$ such that no edge appears twice and $e_k = e_{\ell+1}$. Thus W ends periodically on the sequence of edges $e_k, \ldots, e_\ell$. By Lemma 14, all the closed walks that are part of $\widetilde{F}$ have some outgoing incident edges of D on their left side. Thus we have that W' contains at least one edge that is not an edge of $\widetilde{F}$, thus it contains at least one rigid edge.

By construction, on the left side of W', there is no incident outgoing edges of D. So, by Lemma 14, W' is a triangle with its interior on its left side. So W' is a 0-homologous oriented subgraph of D, thus all its edges are non-rigid by Lemma 11, a contradiction. □

By Lemma 15, every face of $\widetilde{G}$ is quasi-contractible and its outer facial walk is a triangle. So $\widetilde{G}$ contains all the triangles of G whose interiors are maximal by inclusion, i.e. it contains all the edges that are not in the interior of a separating triangle. In particular, $\widetilde{G}$ is non-empty and $|O(G)| \geq 2$. The status (rigid or not) of an edge lying inside a separating triangle is determined as in the planar case: such an edge is rigid if and only if it is in the interior of a separating triangle and incident to this triangle. Thus an edge of G is rigid if and only if it is in the interior of a separating triangle and incident to this triangle.

Since $(O(G), \leq_{f_0})$ is a distributive lattice, any element D of $O(G)$ that is distinct from $D_{\max}$ and $D_{\min}$ contains at least one neighbor above and at least one neighbor below in the Hasse diagram of the lattice. Thus it has at least one face of $\widetilde{G}$ oriented counterclockwise and at least one face of $\widetilde{G}$ oriented clockwise. Thus by Lemma 15, it contains at least one triangle oriented counterclockwise and at least one triangle oriented clockwise. Next lemma shows that this property is also true for $D_{\max}$ and $D_{\min}$.

Lemma 16 *In $D_{\max}$ (resp. $D_{\min}$) there is a counterclockwise (resp. clockwise) triangle containing f_0, and a clockwise (resp. counterclockwise) triangle not containing f_0.*

Proof By Lemma 15, $\widetilde{f_0}$ is quasi-contractible and its outer facial walk is a triangle T. By lemma 13, $\widetilde{F_0}$ is an oriented subgraph of $D_{\max}$. Thus T is oriented counterclockwise and contains f_0. The second part of the lemma is clear since $|O(G)| \geq 2$ so $D_{\max}$ has at least one neighbor below in the Hasse diagram of the lattice. Similarly for $D_{\min}$. □

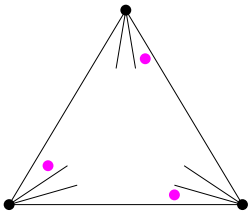

Fig. 20 Angles that are in a separating triangle but not in its clockwise interior

Thus by above remarks and Lemma 16, all the HTC Schnyder woods have at least one triangle oriented counterclockwise and at least one triangle oriented clockwise. Note that this property does not characterize HTC Schnyder woods. Figure 7 gives an example of a Schnyder wood that is not HTC but satisfies the property. Note also that not all Schnyder woods satisfy the property. The right of Fig. 5 is an example of a Schnyder wood that is no HTC and has no oriented triangle.

Lemma 16 is used in the next section to obtained a bijection with unrooted unicellular maps.

11 Bijection with Unrooted Unicellular Maps

To remove the root and the balanced property of the unicellular maps considered in Theorem 6, we have to root the toroidal triangulation more precisely than before. We say that an angle is not *in the clockwise interior of a separating triangle* if it is not in its interior, or if it is incident to a vertex v of the triangle and situated just before an edge of the triangle in counterclockwise order around v (see Fig. 20).

Consider a toroidal triangulation G. Consider a root angle a_0 that is not in the clockwise interior of a separating triangle. Note that the choice of a_0 is equivalent to the choice of a root vertex v_0 and a root edge e_0 incident to v_0 such that none is in the interior of a separating triangle. Consider the orientation of the edges of G corresponding to the minimal HTC Schnyder wood w.r.t. the root face f_0. By Lemma 16, there is a clockwise triangle containing f_0. Thus by the choice of a_0, the edge e_0 is leaving the root vertex v_0. This is the essential property used in this section. Consider the output U of ALGORITHM PS on (G, a_0). Since e_0 is leaving v_0 and a_0 is just before e_0 in counterclockwise order around v_0, the execution of ALGORITHM PS starts by Case 2 and e_0 corresponds in U to a stem s_0 attached to v_0. We call this stem s_0 the *root stem*.

The recovering method defined in Theorem 4 says that s_0 is the last stem reattached by the procedure. So there exists a sequence of admissible triples of U (see the terminology and notations of Sect. 6) such that s_0 belongs to the last admissible triple. Let $U_0 = U$ and for $1 \leq k \leq 2n-2$, the map U_k is obtained from U_{k-1} by closing any admissible triple that does no contain s_0. As noted in Sect. 6, the special face of U_{2n-2} is a quadrangle with exactly one stem. This stem being s_0, we are in the situation of Fig. 21.

Consequently, if one removes the root stem s_0 from U to obtain a unicellular map U' with n vertices, $n+1$ edges and $2n-2$ stems, one can recover the graph U_{2n-2} by applying a complete closure procedure on U' (see example of Fig. 22). Note that then,

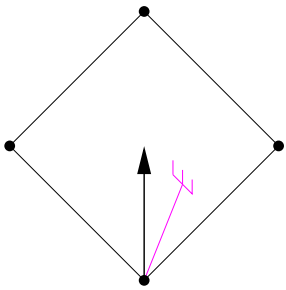

Fig. 21 The situation just before the last stem (i.e. the root stem) is reattached

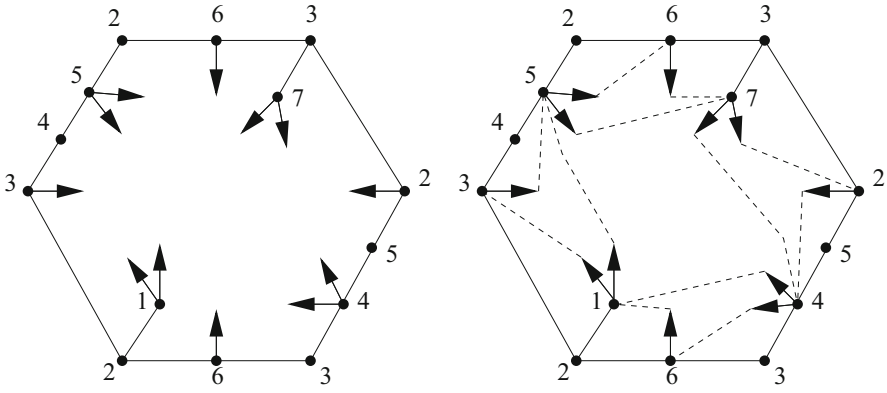

Fig. 22 Example of K_7 where the root angle, the root stem and the orientation w.r.t. the root angle have been removed from the output of Fig. 9. The complete closure procedure leads to a quadrangular face

there are four different ways to finish the closure of U_{2n-2} to obtain an oriented toroidal triangulation. This four cases correspond to the four ways to place the (removed) root stem in a quadrangle, they are obtained by pivoting Fig. 21 by 0°, 90°, 180° and 270°. Note that only one of this four cases leads to the original rooted triangulation G, except if there are some symmetries (like in the example of Fig. 22).

Let $\mathcal{U}(n)$ denote the set of (non-rooted) toroidal unicellular maps, with exactly n vertices, $n+1$ edges and $2n-2$ stems satisfying the following: a vertex has exactly 2 stems if it is not a corner, 1 stem if it is the corner of an hexagon and 0 stem if it is the corner of a square. Note that the output of Theorem 3 on an appropriately rooted toroidal triangulation is an element of $\mathcal{U}(n)$ when the root stem is removed.

Note that an element U' of $\mathcal{U}(n)$ is non-rooted so we cannot orient automatically its edges w.r.t. the root angle like in Sect. 9. Nevertheless one can still orient all the stems as outgoing and compute γ on the cycles of U' by considering only its stems in the counting (and not the edges nor the root stem anymore). We say that a unicellular map of $\mathcal{U}(n)$ satisfies the γ_0 property if γ equals zero on its (non-contractible) cycles. Let us call $\mathcal{U}_{\gamma_0}(n)$ the set of elements of $\mathcal{U}(n)$ satisfying the γ_0 property.

A surprising property is that an element U' of $\mathcal{U}(n)$ satisfies the γ_0 property if and only if any element U of $\mathcal{U}_r(n)$ obtained from U' by adding a root stem anywhere in U'

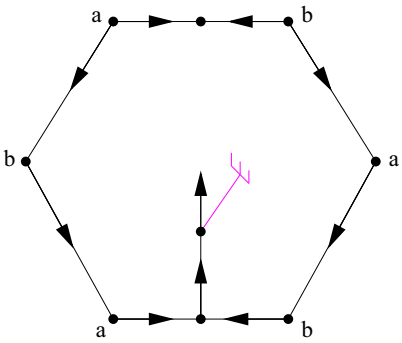

Fig. 23 The parts of the unicellular map showing the correspondence while computing γ with or without the orientation w.r.t. the root plus the root stem

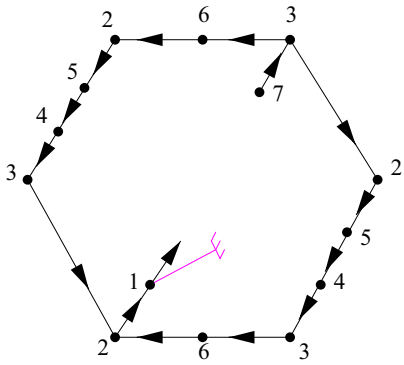

Fig. 24 The difference between the rooted output of Fig. 9 and the non-rooted output of Fig. 22

satisfies the γ_0 property (note that in U we count the edges and the root stem to compute γ). One can see this by considering the unicellular map of Fig. 23. It represents the general case of the underlying rooted hexagon of U. The edges represent in fact paths (some of which can be of length zero). One can check that it satisfies γ equals zero on its (non-contractible) cycles. It corresponds exactly to the set of edges that are taken into consideration when computing γ on U but not when computing γ on U'. Thus it does not affect the counting (the tree-like parts are not represented since they do not affect the value γ). So the output of Theorem 3 on an appropriately rooted toroidal triangulation is an element of $\mathcal{U}_{\gamma_0}(n)$ when the root stem is removed.

For the particular case of K_7, the difference between the rooted output of Fig. 9 and the non-rooted output of Fig. 22 is represented in Fig. 24 (one can superimpose the last two to obtain the first). One can check that these three unicellular maps (rooted, non-rooted and the difference) all satisfy γ equals zero on their cycles.

There is an "almost" four-to-one correspondence between toroidal triangulations on n vertices, given with a root angle that is not in the clockwise interior of a separating triangle, and elements of $\mathcal{U}_{\gamma_0}(n)$. The "almost" means that if the automorphism group of an element U of $\mathcal{U}_{\gamma_0}(n)$ is not trivial, some of the four ways to add a root stem in U are isomorphic and lead to the same rooted triangulation. In the example of Fig. 22, one can root in four ways the quadrangle but this gives only two different rooted

triangulations (because of the symmetries of K_7). We face this problem by defining another class for which we can formulate a bijection.

Let $\mathcal{T}(n)$ be the set of toroidal maps on n vertices, where all the faces have length three, except one that has length four and which is not in a separating triangle. Then we have the following bijection:

Theorem 7 *There is a bijection between $\mathcal{T}(n)$ and $\mathcal{U}_{\gamma_0}(n)$.*

Proof Let a (for "add") be an arbitrarily chosen mapping defined on the maps G' of $\mathcal{T}(n)$ that adds a diagonal e_0 in the quadrangle of G' and roots the obtained toroidal triangulation G at a vertex v_0 incident to e_0 (this defines the root angle a_0 situated just before e_0 in counterclockwise order around v_0). Note that the added edge cannot create homotopic multiple edges, since otherwise the quadrangle would be in a separating triangle. Moreover the root angle of G is not in the clockwise interior of a separating triangle. Thus the image of a is in $\mathcal{T}'_r(n)$, the subset of $\mathcal{T}_r(n)$ corresponding to toroidal triangulations rooted at an angle that is not in the clockwise interior of a separating triangle.

Let $\mathcal{U}'_{r,b,\gamma_0}(n)$ be the elements of $\mathcal{U}_{r,b,\gamma_0}(n)$ that have their root angle just before a stem in counterclockwise order around the root vertex. Consider the mapping g, defined in the proof of Theorem 9. By above remarks and Theorem 9, the image of g restricted to $\mathcal{T}'_r(n)$ is in $\mathcal{U}'_{r,b,\gamma_0}(n)$. Let r (for "remove") be the mapping that associates to an element of $\mathcal{U}'_{r,b,\gamma_0}(n)$ an element of $\mathcal{U}_{\gamma_0}(n)$ obtained by removing the root angle and its corresponding stem. Finally, let $h = r \circ g \circ a$ which associates to an element of $\mathcal{T}(n)$ an element of $\mathcal{U}_{\gamma_0}(n)$. Let us show that h is a bijection.

Consider an element G' of $\mathcal{T}(n)$ and its image U' by h. The complete closure procedure on U' gives G' thus the mapping h is injective.

Conversely, consider an element U' of $\mathcal{U}_{\gamma_0}(n)$. Apply the complete closure procedure on U'. At the end of this procedure, the special face is a quadrangle whose angles are denoted $\alpha^1, \ldots, \alpha^4$. We denote also by $\alpha^1, \ldots, \alpha^4$ the corresponding angles of U'. For $i \in \{1, \ldots, 4\}$, let U^i be the element of $\mathcal{U}_r(n)$ obtained by adding a root stem and a root angle in the angle α^i of U', with the root angle just before the stem in counterclockwise order around the root vertex. Note that by the choice of α^i, the U^i are all balanced. By above remarks they also satisfy the γ_0 property and thus they are in $\mathcal{U}'_{r,b,\gamma_0}(n)$.

By the proof of Theorem 6, the complete closure procedure on U^i gives a triangulation G^i of $\mathcal{T}_r(n)$ that is rooted from an angle a_0^i not in the strict interior of a separating triangle and oriented according to the minimal HTC Schnyder wood w.r.t. the root face. Moreover the output of ALGORITHM PS applied on (G^i, a_0^i) is U^i. Since in U^i, the root stem is present just after the root angle, the first edge seen by the execution of ALGORITHM PS on (G^i, a_0^i) is outgoing. So a_0 is not in the clockwise interior of a separating triangle (in a 3-orientation, all the edges that are in the interior of a separating triangle and incident to the triangle are entering the triangle). Thus the G^i are appropriately rooted and are elements of $\mathcal{T}'_r(n)$. Removing the root edge of any G_i, gives the same map G' of $\mathcal{T}(n)$. Exactly one of the G_i is the image of G' by the mapping a. Thus the image of G' by h is U' and the mapping h is surjective. □

A nice aspect of Theorem 7 comparing to Theorem 6 is that the unicellular maps that are considered are much simpler. They have no root nor balanced property anymore. It would be great to use Theorem 7 to count and sample toroidal triangulations. The main issue comparing to the planar case seems to be the γ_0 property.

12 Conclusion

Note that the work presented here is related to a work of Bernardi and Chapuy [5] (their convention for the orientation of the edges is the reverse of ours). Consider a map G (not necessarily a triangulation) on an oriented surface of genus g, rooted at a particular angle a_0. An orientation of G is *right* if for each edge e, the *right-walk* starting from e (when entering a vertex, the next chosen edge is the one leaving on the right) reaches the root edge e_0 via the root vertex v_0. A consequence of [5] is that ALGORITHM PS applied on an orientation of (G, a_0) outputs a spanning unicellular submap U if and only if the considered orientation is right. Note that in this characterization, the submap U is not necessarily a map of genus g, its genus can be any value in $\{0, \ldots, g\}$. In the particular case of toroidal triangulations we show that by considering minimal HTC Schnyder woods the output U is a toroidal spanning unicellular map. Hence by the above characterization, minimal HTC Schnyder woods are right. But here, the fact that U and G have the same genus is of particular interest as it yields a simple bijection.

The key property that makes U and G have same genus is the conclusion of Lemma 2 (no oriented non-contractible cycle in the dual orientation). Recently, Albar, the second author and Knauer [1] proved the following:

Theorem 8 ([1]) *A simple triangulation on a genus $g \geq 1$ orientable surface admits an orientation of its edges such that every vertex has outdegree at least* 3*, and divisible by* 3.

Theorem 8 is proved for simple triangulation but we believe it to be true for all triangulations. Moreover we hope for a possible generalization satisfying the conclusion of Lemma 2:

Conjecture 1 *A triangulation on a genus $g \geq 1$ orientable surface admits an orientation of its edges such that every vertex has outdegree at least* 3*, divisible by* 3*, and such that there is no oriented non-contractible cycle in the dual orientation.*

If Conjecture 1 is true, one can consider a minimal orientation satisfying its conclusion and apply ALGORITHM PS to obtain a unicellular map of the same genus as G. Note that more efforts should be made to obtain a bijection since there might be several minimal elements satisfying the conjecture and a particular one has to be identified (as the minimal HTC Schnyder wood in our case).

Acknowledgments We thank Luca Castelli Aleardi, Nicolas Bonichon, Eric Fusy and Frédéric Meunier for fruitful discussions about this work. This work was supported by the Grant EGOS ANR-12-JS02-002-01 and the project-team GALOIS supported by LabEx PERSYVAL-Lab ANR-11-LABX-0025.

References

1. Albar, B., Gonçalves, D., Knauer, K.: Orienting triangulations. J. Graph Theory **83**(4), 392–405 (2016)
2. Albenque, M., Poulalhon, D.: Generic method for bijections between blossoming trees and planar maps. Electron. J. Comb. **22**(2), paper P2.38 (2015)
3. Aleardi, L.C., Fusy, E., Lewiner, T.: Optimal encoding of triangular and quadrangular meshes with fixed topology. In: Proceedings of the 22nd Canadian Conference on Computational Geometry (CCCG 2010)
4. Bernardi, O.: Bijective counting of tree-rooted maps and shuffles of parenthesis systems. Electron. J. Comb. **14**, R9 (2007)
5. Bernardi, O., Chapuy, G.: A bijection for covered maps, or a shortcut between Harer-Zagier's and Jackson's formulas. J Comb Theory A **118**, 1718–1748 (2011)
6. Bonichon, N., Gavoille, C., Hanusse, N.: An information-theoretic upper bound of planar graphs using triangulation. Proceedings of the 20th Annual Symposium on Theoretical Aspects of Computer Science (STACS 2003). Lecture Notes in Computer Science, vol. 2607, pp. 499–510. Springer, Berlin (2003)
7. Chapuy, G.: A new combinatorial identity for unicellular maps, via a direct bijective approach. Adv. Appl. Math. **47**, 874–893 (2011)
8. Chapuy, G., Marcus, M., Schaeffer, G.: A bijection for rooted maps on orientable surfaces. SIAM J. Discrete Math. **23**, 1587–1611 (2009)
9. de Fraysseix, H., de Mendez, O.P.: On topological aspects of orientations. Discrete Math. **229**, 57–72 (2001)
10. de Mendez, P.O.: Orientations bipolaires. PhD Thesis (1994)
11. Duchi, E., Poulalhon, D., Schaeffer, G.: Uniform random sampling of simple branched coverings of the sphere by itself. In: Proceedings of the Twenty-Fifth Annual ACM-SIAM Symposium on Discrete Algorithms. pp. 294–304. Society for Industrial and Applied Mathematics, New York (2013)
12. Felsner, S.: Lattice structures from planar graphs. Electron. J. Comb. **11**, R15 (2004)
13. Fusy, E.: Combinatoire des cartes planaires et applications algorithmiques. PhD Thesis (2007). http://www.lix.polytechnique.fr/Labo/Eric.Fusy/Theses/these_eric_fusy.pdf
14. Giblin, P.: Graphs. Surfaces and Homology. Cambridge University Press, Cambridge (2010)
15. Gonçalves, D., Lévêque, B.: Toroidal maps: Schnyder woods, orthogonal surfaces and straight-line representations. Discrete Comput. Geom. **51**, 67–131 (2014)
16. Gonçalves, D., Knauer, K., Lévêque, B.: Structure of Schnyder labelings on orientable surfaces (2015). arXiv:1501.05475
17. Kant, G.: Drawing planar graphs using the canonical ordering. Algorithmica **16**, 4–32 (1996)
18. Lévêque, B.: Generalization of Schnyder woods to orientable surfaces and applications. HDR Thesis (2016). http://pagesperso.g-scop.grenoble-inp.fr/~levequeb/Publications/HDR.pdf
19. Mohar, B.: Straight-line representations of maps on the torus and other flat surfaces. Discrete Math. **155**, 173–181 (1996)
20. Poulalhon, D., Schaeffer, G.: Optimal coding and sampling of triangulations. Algorithmica **46**, 505–527 (2006)
21. Propp, J.: Lattice structure for orientations of graphs (1993). arXiv:math/0209005
22. Schnyder, W.: Planar graphs and poset dimension. Order **5**, 323–343 (1989)
23. Ueckerdt, T.: Geometric representations of graphs with low polygonal complexity. PhD Thesis (2011). http://www.math.kit.edu/iag6/~ueckerdt/media/thesis-ueckerdt.pdf